Research Square

Preprints are preliminary reports that have not undergone peer review.
They should not be considered conclusive, used to inform clinical practice,
or referenced by the media as validated information.

# MIR-129 and MIR-182 Suppress Aggressiveness of Fetal Alcohol Induced Pituitary Neuroendocrine Tumors

**Omkaram Gangisetty**
Rutgers, The State University of New Jersey
**Dipak K. Sarkar**
Dipak.sarkar@rutgers.edu
Rutgers, The State University of New Jersey

**Article**

**Keywords:** Prenatal alcohol exposure, miR-129, miR-182, neuroendocrine tumors

**Posted Date:** November 18th, 2026

**DOI:** https://doi.org/10.21203/rs.3.rs-11460067/v1

**License:** This work is licensed under a Creative Commons Attribution 4.0 International License.
Read Full License

**Additional Declarations:**
No competing interests reported.

Tables 1 and 2 are available in the Supplementary Files section.

# MIR-129 AND MIR-182 SUPPRESS AGGRESSIVENESS OF FETAL ALCOHOL INDUCED PITUITARY NEUROENDOCRINE TUMORS

Omkaram Gangisetty, Dipak K Sarkar

The Endocrine Program, Department of Animal Sciences, Rutgers, The State University of New Jersey, 67 Poultry Lane, New Brunswick, NJ 08901.

Corresponding author: Dipak K. Sarkar, Endocrine Research Building, 67 Poultry Farm Lane, New Brunswick, NJ 08901; telephone - 848-932-1529; email - Dipak.sarkar@rutgers.edu

Running Title: Pituitary tumor suppressor miRNAs

Key words: Prenatal alcohol exposure, miR-129, miR-182, neuroendocrine tumors.

Grant support: This work was supported by a National Institutes of Health Grant R01AA11591.

Disclosure summary: All authors reported no financial interests or potential conflicts of interest.

## Abstract

Pituitary neuroendocrine tumors (PitNETs) often recur or resist therapy. We previously showed that prenatal alcohol exposure (PAE) promotes aggressive PitNET development, but the underlying mechanisms remain unclear. Here, we investigated the role of microRNAs (miRNAs) in PAE-associated PitNET aggressiveness using pituitary tumor cells from rats exposed prenatally to alcohol (AF) or control diet (AD). miRNA profiling identified significant downregulation of miR-129, miR-182, and miR-499 in AF tumor cells. Transient or stable overexpression of miR-129 and miR-182 suppressed AF cell proliferation, migration, and colony formation, whereas miR-499 primarily reduced migration. In xenograft models, AF cells stably overexpressing miR-129 or miR-182 produced significantly smaller tumors, confirming their tumor-suppressive effects in vivo. Mechanistically, miR-129 reduced WNT-5A and MMP-19 expression, while miR-182 decreased VEGF-C and VEGFR3 expression. Luciferase reporter assays confirmed direct interactions of miR-129 and miR-182 with the 3′UTRs of *WNT5A* and *VEGFC*, respectively. These findings identify miR-129 and miR-182 as tumor-suppressive miRNAs whose downregulation contributes to PAE-associated PitNET aggressiveness and suggest that restoring their activity may provide a potential therapeutic strategy for aggressive PitNETs.

## Introduction

Pituitary neuroendocrine tumors (PitNETs) are common intracranial tumors, with prolactinomas accounting for approximately 40% of all pituitary tumors. We previously reported that PAE increases pituitary tumor development following estrogen treatment. PAE-induced pituitary tumors exhibit aggressive characteristics, including extensive invasion into surrounding tissues and distant metastasis (Jabbar et al., 2018). Genetic and epigenetic alterations have been implicated in the development and progression of aggressive pituitary tumors (Ezzat and Asa, 2006; Yoshino et al., 2007). Aberrant DNA methylation may also contribute to the development of alcohol-induced aggressive pituitary tumors (Yoshino et al., 2007; Gangisetty et al., 2015). More recently, we demonstrated a role for developmental pluripotency-associated 4 (DPPA4) in promoting tumor stemness and aggressiveness in PAE-induced pituitary tumors (Chaudhary et al., 2025).

MicroRNAs (miRNAs) represent another important class of epigenetic regulators involved in tumor pathogenesis. Approximately 50% of miRNAs are located within cancer-associated fragile genomic regions (Calin et al., 2004). Dysregulation of miRNA expression is closely associated with cancer initiation, progression, invasion, and metastasis. Upregulated miRNAs may function as oncogenic miRNAs, or oncomiRs, through gain-of-function mechanisms, whereas downregulated miRNAs may function as tumor suppressors, whose loss promotes tumor growth. Numerous tumor-suppressive miRNAs are aberrantly downregulated in cancer and regulate cellular processes such as proliferation (Mohammadi-Yeganeh et al., 2016), apoptosis (Liu et al., 2021; Elnaggar et al., 2021), and epithelial-to-mesenchymal transition (EMT) (Lamouille et al., 2014). Growing evidence also indicates that aberrant miRNA expression contributes to pituitary tumor development (Mao et al., 2010; Bottoni et al., 2007). Both oncogenic and tumor-suppressive miRNAs have been identified in different types of pituitary tumors (Palumbo et al., 2013; Grzywa et al., 2019; Renjie and Haiqian, 2015). However, miRNA

dysregulation and its functional significance in PAE-induced aggressive pituitary tumors remain largely unknown.

In the present study, we used a TaqMan-based TILDA array to determine miRNA expression profiles in cells derived from pituitary tumors of AF rats compared with those from control AD rats. We identified three miRNAs—miR-129, miR-182, and miR-499—that were markedly downregulated in AF cells. These miRNAs have previously been reported to be downregulated in several types of cancer (Yu et al., 2015; Jiang et al., 2016; Ma et al., 2015; Zeng et al., 2018; Li et al., 2018; Jia et al., 2019; Yan et al., 2020; Ma et al., 2021; Wang et al., 2020); however, their potential tumor-suppressive roles in PAE-induced PitNETs have not been investigated. We found that miR-129, miR-182, and miR-499 were downregulated in AF rat pituitary tumor cells and tissues compared with controls. Functional studies demonstrated that miR-129 and miR-182 suppressed the proliferation, colony formation, and migration of AF cells, whereas miR-499 had little or no effect on proliferation or colony formation. Furthermore, stable overexpression of miR-129 or miR-182 reduced tumor development in a mouse xenograft model. Mechanistically, we identified WNT-5A and MMP-19 as targets regulated by miR-129 and VEGF-C and VEGFR-3 as targets regulated by miR-182. Luciferase reporter assays further demonstrated the direct regulation of WNT-5A by miR-129 and VEGF-C by miR-182. Together, these findings identify miR-129 and miR-182 as potential tumor suppressors in PAE-induced aggressive PitNETs.

## Results

### Prenatal Alcohol Exposure Alters the miRNA Expression Profile of Pituitary Tumor-Derived Cells

We previously reported that pituitary tumors from estrogen-treated AF rats were larger, hemorrhagic, and more invasive, including penetration into the sphenoid bone, compared with tumors from control AD rats (Jabbar et al., 2018; Chaudhary et al., 2025). Cells isolated from

AD and AF pituitary tumors also exhibited distinct morphological and functional characteristics. AD cells were rounded, partially attached, and slow-growing, whereas AF cells exhibited a polygonal morphology, were firmly attached, and grew rapidly (Fig. 1A). Cell proliferation was significantly increased in AF cells compared with AD cells (Fig. 1B). Colony formation and migration assays further demonstrated that AF cells formed more colonies and exhibited greater migratory activity than AD cells (Fig. 1C, D), confirming the highly tumorigenic phenotype of AF cells.

To determine whether altered miRNA expression was associated with this aggressive phenotype, we analyzed miRNA expression using a TaqMan-based TILDA array containing 384 miRNAs. Differential miRNA expression was visualized by plotting log2 fold change against −log2(*p* value) (Fig. 1E). Using a threshold of ≥10-fold change and $p < 0.05$, we identified 17 upregulated and three downregulated miRNAs in AF cells compared with AD cells. Differentially expressed miRNAs were also visualized using a heat map (Fig. 1F). Among the downregulated miRNAs, miR-129, miR-182, and miR-499 were selected for further investigation. Because the loss of tumor-suppressive miRNAs can contribute to cancer progression, we hypothesized that reduced expression of these miRNAs may contribute to the aggressive phenotype of AF pituitary tumor cells.

**PAE Reduces miR-129, miR-182, and miR-499 Expression in Rat Pituitary Tumor Cells and Tissues**

Genome-wide miRNA profiling identified miR-129, miR-182, and miR-499 as markedly downregulated in AF pituitary tumor cells compared with AD control cells. We validated these findings using individual TaqMan miRNA assays. Expression of miR-129, miR-182, and miR-499 was markedly reduced in AF pituitary tumor cells compared with AD cells (Fig. 2A–C), with expression levels reduced by approximately 10- to 100-fold. We next examined the expression of these miRNAs in pituitary tumor tissues. Consistent with the cell-culture findings, miR-129,

miR-182, and miR-499 expression was significantly reduced in AF pituitary tumor tissues compared with AD and PF control tissues (Fig. 2D–F). The magnitude of miRNA downregulation was less pronounced in tumor tissues than in cultured tumor cells, potentially reflecting the cellular heterogeneity of intact tumor tissues. Together, these findings demonstrate that PAE is associated with reduced expression of miR-129, miR-182, and miR-499 in both pituitary tumor cells and tumor tissues.

**miR-129 and miR-182 Overexpression Suppresses Tumorigenic Features of AF Rat Pituitary Tumor Cells**

AF rat pituitary tumor cells exhibit a highly tumorigenic phenotype characterized by increased proliferation, colony formation, and migration. We previously demonstrated that transplantation of AF pituitary tumor cells into immunodeficient mice results in larger tumors than transplantation of control AD cells (Jabbar et al., 2018). Because miR-129, miR-182, and miR-499 were markedly downregulated in AF cells, we investigated whether restoring their expression could suppress the tumorigenic phenotype. AF cells were transfected with miR-129, miR-182, or miR-499 mimic oligonucleotides or a negative-control mimic. TaqMan assays confirmed robust increases in the corresponding miRNA following mimic transfection (Figs. 3A, 4A, and 5A). Cell proliferation was assessed using the MTT assay. Overexpression of miR-129 or miR-182 significantly reduced AF cell proliferation in a time-dependent manner compared with untreated and negative-control mimic-treated cells (Figs. 3B and 4B). In contrast, miR-499 overexpression did not significantly alter cell proliferation (Fig. 5B). Similarly, overexpression of miR-129 or miR-182 significantly reduced colony formation compared with untreated and negative-control mimic-treated AF cells (Figs. 3C, D and 4C, D), whereas miR-499 overexpression did not significantly affect colony formation (Fig. 5C, D). Transwell migration assays demonstrated that overexpression of miR-129, miR-182, or miR-499 significantly reduced AF cell migration compared with control and negative-control mimic-treated cells (Figs.

3–5E, F). Together, these findings demonstrate that miR-129 and miR-182 suppress multiple tumorigenic characteristics of AF pituitary tumor cells, including proliferation, colony formation, and migration. In contrast, miR-499 primarily affected cell migration without significantly altering proliferation or colony formation.

**Stable Overexpression of miR-129 or miR-182 Suppresses AF Pituitary Tumor Development In Vivo**

We next investigated whether the tumor-suppressive effects of miR-129 and miR-182 observed in vitro were maintained in vivo using a xenograft model. Stable AF cell lines overexpressing miR-129 or miR-182 were generated using pCMV-miR expression vectors (Fig. 6A). TaqMan assays confirmed robust overexpression of miR-129 or miR-182 in the corresponding stable cell lines compared with AF control and vector-control cells (Fig. 6B, C). Consistent with the transient-transfection experiments, stable overexpression of either miR-129 or miR-182 significantly reduced AF cell proliferation compared with control and vector-transfected cells (Fig. 6D, E).

To determine whether these miRNAs suppress tumor development in vivo, AF control cells, vector-control cells, and stable miR-129- or miR-182-overexpressing AF cells were injected into immunodeficient mice. Tumors became detectable approximately 6 days after cell injection and were monitored until the experimental endpoint. AF cells stably overexpressing miR-129 or miR-182 produced significantly smaller tumors than AF control or vector-control cells (Fig. 7A, B). Both tumor volume and tumor wet weight were significantly reduced in mice receiving miR-129- or miR-182-overexpressing AF cells (Fig. 7C, D). These findings provide in vivo evidence supporting the tumor-suppressive roles of miR-129 and miR-182 in PAE-associated aggressive pituitary tumor cells.

**miR-129 Regulates WNT-5A and MMP-19 in AF Pituitary Tumor Cells**

We next investigated the molecular mechanisms through which miR-129 suppresses the tumorigenic phenotype of AF rat pituitary tumor cells. Three bioinformatic prediction tools—TargetScan, PicTar, and miRDB were used to identify potential miR-129 target genes. Predicted targets included members of the SOX, MMP, WNT, and KLF gene families (Supplementary Table 1). Previous studies have demonstrated that miR-129 targets WNT-5A in glioblastoma and vascular smooth muscle cells (Zeng et al., 2018; Zhang et al., 2016). miR-129 has also been reported to regulate MMP9 in non-small-cell lung cancer (Li et al., 2015). AF pituitary tumor cells were transfected with miR-129 mimic, and increased miR-129 expression was confirmed using a TaqMan miRNA assay (Fig. 3A). We subsequently examined the expression of selected predicted target genes. miR-129 overexpression significantly reduced SOX2, MMP-19, and WNT-5A expression compared with mock-control and negative-control mimic-treated cells (Fig. 8A, B, D). In contrast, BCL2 and KLF7 expression was not significantly altered (Fig. 8C, E). Western blot analysis further demonstrated that WNT-5A and MMP-19 protein levels were significantly reduced following miR-129 overexpression (Fig. 8F, G). Together, these findings suggest that miR-129 suppresses tumorigenic properties of AF pituitary tumor cells, at least in part, through regulation of WNT-5A and MMP-19 expression.

**miR-182 Regulates VEGF Signaling in AF Pituitary Tumor Cells**

We next investigated the mechanisms through which miR-182 suppresses the tumorigenic phenotype of AF rat pituitary tumor cells. TargetScan, PicTar, and miRDB were used to identify potential miR-182 target genes, including members of the SOX, MMP, BCL2, WNT, and KLF families (Supplementary Table 1). Previous studies have shown that miR-182 is downregulated in colon cancer and can suppress tumor growth by targeting VEGF-C (Yan et al., 2020). We therefore transfected AF cells with miR-182 mimic and examined the expression of selected candidate targets. miR-182 overexpression significantly reduced VEGF-C and VEGF-R3 mRNA expression compared with mock-control and negative-control mimic-treated cells (Fig. 9G, I). In

contrast, expression of SOX2, MMP16, BCL2, WNT-5A, KLF7, VEGF-A, and VEGF-D was not significantly altered (Fig. 9A–F, H). Western blot analysis confirmed significant reductions in VEGF-C and VEGF-R3 protein levels in AF cells overexpressing miR-182 (Fig. 9J, K). These findings suggest that miR-182 suppresses the tumorigenic properties of AF pituitary tumor cells, at least in part, through inhibition of VEGF-C/VEGF-R3 signaling.

### miR-129 Directly Targets the WNT-5A 3′UTR, Whereas miR-182 Directly Targets the VEGF-C 3′UTR

Our findings demonstrated that miR-129 reduced WNT-5A and MMP-19 expression, whereas miR-182 reduced VEGF-C and VEGF-R3 expression. We next investigated whether these miRNAs directly interact with predicted binding sites within the 3′UTRs of their target genes. The rat WNT-5A and VEGF-C 3′UTRs containing their respective predicted miRNA-binding sites were cloned downstream of Renilla luciferase in the psiCHECK-2 reporter vector. Firefly luciferase served as an internal normalization control (Fig. 10A). HEK293 cells were co-transfected with the reporter constructs and either miR-129 mimic, miR-182 mimic, or negative-control mimic. miR-129 significantly reduced luciferase activity of the WNT-5A 3′UTR reporter compared with the negative-control mimic (Fig. 10B). Similarly, miR-182 significantly reduced luciferase activity of the VEGF-C 3′UTR reporter (Fig. 10C). These results support direct regulation of WNT-5A by miR-129 and VEGF-C by miR-182 through interactions with their binding sites of respective 3′UTRs.

## Discussion

We previously demonstrated that PAE increases the aggressiveness of pituitary tumor development following estrogen treatment in both male and female rats. Pituitary tumor cells derived from AF rats proliferate rapidly, form numerous colonies, exhibit increased migration,

and produce tumors following transplantation into immunodeficient mice, supporting their highly tumorigenic phenotype. These cells also exhibit elevated expression of stem cell-associated proteins and DPPA4, a regulator of stem cell properties. We further demonstrated that DPPA4 increases the expression of genes associated with tumor aggressiveness and promotes the tumorigenic potential of pituitary tumor cells (Jabbar et al., 2018; Chaudhary et al., 2025, 2026). However, the molecular mechanisms through which PAE promotes aggressive pituitary tumor development remain incompletely understood. Genetic and epigenetic alterations contribute to the development and progression of aggressive pituitary tumors (Ezzat and Asa, 2006; Yoshino et al., 2007). Aberrant DNA methylation has also been implicated in alcohol-associated aggressive pituitary tumor development (Yoshino et al., 2007; Gangisetty et al., 2015). In addition to DNA methylation, miRNAs represent an important epigenetic regulatory mechanism controlling tumor initiation, progression, invasion, and metastasis (Mao et al., 2010; Bottoni et al., 2007). Numerous miRNAs function as tumor suppressors, and their downregulation can disrupt cellular processes controlling proliferation, apoptosis, migration, invasion, and metastasis. For example, miR-15/16 are downregulated in several solid tumors, including melanoma, bladder cancer, colorectal cancer, pituitary adenomas, and prostate cancer, and exert tumor-suppressive effects primarily through regulation of BCL2 (Pekarsky and Croce, 2015; Cimmino et al., 2005). The miR-200 family represents another important group of tumor-suppressive miRNAs that regulate EMT by directly targeting ZEB1 and ZEB2 (Gregory et al., 2008; Title et al., 2018). Similarly, miR-340 inhibits breast cancer metastasis through regulation of WNT signaling (Mohammadi-Yeganeh et al., 2016). Tumor-suppressive miRNAs have also been identified in several types of pituitary tumors (Renjie and Haiqian, 2015).

Environmental exposures during early development, including alcohol, tobacco smoke, endocrine-disrupting chemicals, prenatal stress, hypoxia, and malnutrition, can alter gene expression through epigenetic mechanisms. Increasing evidence indicates that prenatal exposure to environmental toxicants can alter miRNA expression profiles (Kappil and Chen,

2014). Prenatal alcohol exposure has been associated with differential miRNA expression and fetal abnormalities in experimental models (Wang et al., 2009). Ethanol exposure in mouse cortical neurons downregulated several miRNAs, including miR-9, miR-21, miR-153, and miR-335, which have distinct cellular functions (Sathya et al., 2007). Ethanol exposure has also been reported to increase miR-34a expression in neural crest cells, resulting in reduced EMT and migration through suppression of SNAIL1 (Fan et al., 2022). More recently, our laboratory demonstrated that PAE-induced alterations in miR-383 and miR-384 regulate POMC expression and hypothalamic-pituitary-adrenal axis function (Gangisetty et al., 2023).

Alcohol exposure is also associated with tumor development in several tissues, including breast, prostate, pancreas, and colon (Forsyth et al., 2010; Welsch et al., 2006; Papa et al., 2017). Chronic alcohol consumption has been associated with hyperprolactinemia in humans, nonhuman primates, and laboratory animals (Kornet et al., 1991; De et al., 2002). We previously demonstrated that PAE increases prolactin secretion and reduces dopamine D2 receptor expression in the pituitary gland through a mechanism involving miR-9 (Gangisetty et al., 2017). We also recently demonstrated that alcohol exposure during fetal development promotes the formation of aggressive, highly vascularized estrogen-induced pituitary tumors that invade the sphenoid bone.

The present study extends these findings by identifying miR-129 and miR-182 as potential tumor suppressors in PAE-induced aggressive PitNETs. Both miRNAs were markedly downregulated in AF pituitary tumor cells and tissues. Restoration of either miR-129 or miR-182 suppressed cell proliferation, colony formation, and migration in vitro. Furthermore, stable overexpression of either miRNA significantly reduced tumor development in an immunodeficient mouse xenograft model. Together, these results provide functional evidence that loss of miR-129 and miR-182 contributes to the tumorigenic phenotype associated with PAE.

The miR-129 family consists of miR-129-1 and miR-129-2, which share the same seed sequence. Members of the miR-129 family are downregulated in several cancer types and have

been identified as tumor suppressors (Yu et al., 2015; Ma et al., 2017; Liu et al., 2018). Reduced miR-129 expression has also been reported in neuroendocrine tumors (Døssing et al., 2014). Zeng et al. (2018) demonstrated that miR-129 expression is reduced in glioma patient samples and that restoring miR-129 inhibits proliferation, invasion, migration, angiogenesis, and neurosphere formation in glioblastoma cells by directly targeting WNT-5A.

miR-182, a member of the miR-183 family, is dysregulated in multiple cancer types. Depending on the tumor type and signaling pathway involved, miR-182 may function either as a tumor suppressor or as an oncogenic miRNA (Skaftnesmo et al., 2007; Chang et al., 2018; Yan et al., 2020). miR-182 has also been reported to suppress osteosarcoma cell growth and invasion through regulation of TIAM1 and WNT/β-catenin signaling (Hu et al., 2015; Zhang et al., 2017). Other miRNAs, including miR-132 and miR-15a/16, are downregulated in invasive pituitary tumors and suppress proliferation, migration, and invasion (Renjie and Haiqian, 2015). Despite this evidence, the roles of miR-129 and miR-182 in PAE-induced aggressive PitNETs have not previously been defined. Our findings demonstrate that restoration of these miRNAs suppresses the tumorigenic phenotype of AF cells in vitro and reduces tumor growth in vivo. These results therefore identify miR-129 and miR-182 as candidate tumor-suppressive miRNAs in PAE-associated PitNETs.

To investigate the molecular mechanisms underlying these effects, we examined candidate targets of miR-129 and miR-182. Our findings indicate that miR-129 regulates WNT-5A and MMP-19, whereas miR-182 regulates VEGF-C and VEGF-R3. WNT-5A is a ligand involved in noncanonical WNT signaling and plays an important role in tumor progression. We previously reported increased expression of WNT/β-catenin signaling genes in AF rat pituitary tumor cells (Chaudhary et al., 2025). Our present findings are consistent with previous studies demonstrating that miR-129 directly targets WNT-5A and suppresses proliferation, migration, and invasion in glioblastoma cells (Zeng et al., 2018). Matrix metalloproteinases are important mediators of tumor invasion, and increased expression of MMP family members has been

reported in AF rat pituitary tumor cells (Chaudhary et al., 2025). We found that miR-129 overexpression reduced MMP-19 expression, suggesting that suppression of MMP signaling may contribute to the inhibitory effects of miR-129 on AF cell migration and tumorigenicity. Previous studies have similarly demonstrated regulation of MMP9 by miR-129 in non-small-cell lung cancer (Li et al., 2015).

VEGF signaling is a major regulator of angiogenesis and vascular permeability and represents an important therapeutic target in several tumor types. VEGF-C promotes tumor development and lymphangiogenesis through VEGF-C/VEGF-R3 signaling (Yeh et al., 2017). In the present study, miR-182 overexpression reduced both VEGF-C and VEGF-R3 expression. Furthermore, luciferase reporter analysis demonstrated that miR-182 directly interacts with the VEGF-C 3′UTR. These findings are consistent with previous evidence that miR-182 regulates colon cancer tumorigenesis and angiogenesis by targeting VEGF-C (Yan et al., 2020). Our luciferase reporter experiments provide additional mechanistic evidence that miR-129 directly regulates WNT-5A and that miR-182 directly regulates VEGF-C. These findings establish links between the loss of tumor-suppressive miRNAs and activation of signaling pathways involved in tumor growth, migration, invasion, and angiogenesis. Thus, PAE-associated reductions in miR-129 and miR-182 may contribute to the aggressive phenotype of pituitary tumors by releasing inhibitory regulation of WNT/MMP and VEGF signaling pathways.

**Conclusion**

In conclusion, our findings identify miR-129 and miR-182 as tumor-suppressive miRNAs in PAE-induced aggressive pituitary tumors. Both miRNAs are downregulated in AF pituitary tumor cells and tissues, and restoration of their expression suppresses tumorigenic phenotypes in vitro and tumor development in vivo. Mechanistically, miR-129 suppresses WNT-5A and MMP-19 expression, whereas miR-182 suppresses VEGF-C and VEGF-R3 expression. Direct targeting of the WNT-5A and VEGF-C 3′UTRs by miR-129 and miR-182, respectively, was confirmed by

luciferase reporter assays. These findings suggest that loss of miR-129 and miR-182 contributes to PAE-associated pituitary tumor aggressiveness through dysregulation of WNT/MMP and VEGF signaling pathways. Restoration of these tumor-suppressive miRNAs or modulation of their downstream signaling pathways may represent potential therapeutic strategies for aggressive PAE-associated PitNETs.

## Methods

### Animals

Fischer 344 rats (Charles River Laboratories, MA) were housed under controlled environmental conditions (22°C; 12-h light/dark cycle). From gestational day 7 through gestational day 21, pregnant rats were assigned to one of three dietary groups: rat chow provided *ad libitum* (AD), a liquid diet containing ethanol (AF), or an isocaloric pair-fed control liquid diet (PF; Bio-Serv, Frenchtown, NJ). At approximately 60 days of age, female AD, PF, and AF offspring were ovariectomized under sodium pentobarbital anesthesia (50–60 mg/kg, intraperitoneally) and implanted subcutaneously with a 1-cm Silastic capsule (Dow Corning, Midland, MI) containing 17β-estradiol. The estradiol capsule maintained plasma 17β-estradiol concentrations between 120 and 150 pg/mL (De et al., 1995). Pituitary tissues were collected after 120 days of estradiol treatment. For tumor measurements, animals were anesthetized with isoflurane vapors adjusted to 4%using tabletop animal anesthesia system (Harvard apparatus, Holliston, MA) and used for tumor measurements. For tumor tissue collections, animals were euthanized using carbon dioxide for brief unconsciousness followed by rapid decapitation and tissue collections.
All animal surgeries and experimental procedures were performed in accordance with institutional guidelines and NIH policies for the care and use of laboratory animals.
All our animal experimental protocols were approved by Rutgers University Institutional Animal Care Committee (ICAUC) protocol #999900286.

**Rat Pituitary Tumor Cell Culture**

Primary cultures of rat pituitary tumor (RPT) cells were prepared as described previously (Chaudhary et al., 2025; Jabbar et al., 2018). Cells were maintained in DMEM supplemented with 2.5% fetal bovine serum (FBS), 10% horse serum, and 1% penicillin-streptomycin (GIBCO) at 37°C in a humidified incubator containing 7.5% $CO_2$.

**Cell Transfection**

AF rat pituitary tumor cells were cultured in DMEM supplemented with 10% FBS, 5% horse serum, and 1% penicillin-streptomycin (GIBCO). Cells were transfected with miR-129 mimic (MC10195), miR-182 mimic (MC13088), miR-499 mimic (MC11352), or miRNA mimic negative control oligonucleotide #1 (cat. no. 4464058) at a final concentration of 100 nM using Lipofectamine 3000 (Thermo Fisher Scientific, Waltham, MA). All miRNA mimic oligonucleotides were obtained from Thermo Fisher Scientific. Cells were harvested 24 h after transfection for isolation of miRNA, RNA, and protein.

**TaqMan MicroRNA Array**

MicroRNA was extracted from rat pituitary tumor cells using the miRNeasy Kit (Qiagen). TaqMan miRNA array analysis was performed using the TaqMan Rodent MicroRNA Array A according to the manufacturer's instructions (Thermo Fisher Scientific). Arrays were analyzed using a QuantStudio 7 instrument (Thermo Fisher Scientific) and the comparative CT method. Detailed procedures have been described previously (Gangisetty et al., 2023). Briefly, approximately 100 ng of miRNA was reverse-transcribed using the Megaplex RT Reaction Kit. Pre-amplification was performed using Megaplex PreAmp primers and TaqMan PreAmp Master Mix according to the manufacturer's instructions. PCR mixtures were prepared using TaqMan Universal PCR Master Mix and diluted pre-amplified samples. A total of 100 µL of the mixture was loaded into

each port of the TILDA array plate and centrifuged at 1,200 rpm for 1 min. Plates were sealed and amplified using the following conditions: 95°C for 10 min, followed by 40 cycles of 95°C for 15 s and 60°C for 1 min.

**TaqMan MicroRNA Assay**

MicroRNA was extracted from pituitary cells or tissues using the miRNeasy Kit (Qiagen). Approximately 100 ng of miRNA was reverse-transcribed using the TaqMan MicroRNA Reverse Transcription Kit and miRNA-specific RT primers. Reverse transcription was performed using the following program: 16°C for 30 min, 42°C for 30 min, 85°C for 5 min, followed by a hold at 4°C. TaqMan assays were performed using specific assays for miR-129 (ID 000590), miR-182-5p (ID 002599), miR-499 (ID 001352), and U6 snRNA (ID 001973). Mature miRNA sequences are provided in Table 1. All miRNA assay kits were obtained from Thermo Fisher Scientific. Quantitative PCR was performed using TaqMan Gene Expression Master Mix, miRNA-specific TaqMan probes, and cDNA generated with the corresponding miRNA-specific RT primers. Reactions were performed using a QuantStudio 7 instrument under the following conditions: 50°C for 2 min and 95°C for 10 min, followed by 40 cycles of 95°C for 15 s and 60°C for 1 min. Relative miRNA expression was determined using the comparative CT (ΔΔCT) method with U6 snRNA as the reference and calculated as 2^−ΔΔCT.

**Quantitative Real-Time PCR for Gene Expression**

Total RNA was extracted from pituitary cells or tissues using the RNeasy Kit (Qiagen, Germantown, MD) and quantified using a NanoDrop spectrophotometer. One microgram of total RNA was reverse-transcribed using the High-Capacity cDNA Reverse Transcription Kit (Thermo Fisher Scientific). Gene expression was measured by SYBR Green-based quantitative real-time PCR using a QuantStudio 7 instrument. Cycling conditions were 95°C for 5 min, followed by 40 cycles of 95°C for 15 s, 60°C for 30 s, and 72°C for 40 s. Relative expression was calculated

using the ΔΔCT method, with GAPDH as the reference gene (Gangisetty et al., 2023). Primer sequences are provided in Table 2.

**Western Blot Analysis**

Protein levels of WNT-5A, MMP-19, VEGF-C, and VEGF-R3 were determined by Western blot analysis. Total protein was extracted from pituitary cells or tissues and quantified using Bio-Rad protein assay reagents (Bio-Rad, Hercules, CA). Approximately 30 µg of total protein was separated by 12% SDS-PAGE and transferred to PVDF membranes (GE Healthcare, Piscataway, NJ) at 30 V overnight at 4°C. Membranes were blocked in 5% nonfat dry milk prepared in TBS containing 0.1% Tween-20 (TBST) for 3 h at room temperature and incubated overnight at 4°C with primary antibodies in blocking buffer. Primary antibodies included rabbit polyclonal anti-WNT-5A (1:1,000; cat. no. ab227229; Abcam, Cambridge, MA), rabbit polyclonal anti-MMP-19 (1:1,000; cat. no. bs-10058R; Thermo Fisher Scientific), mouse monoclonal anti-VEGF-C (1:750; cat. no. MA5-50861; Thermo Fisher Scientific), rabbit polyclonal anti-VEGF-R3 (1:1,000; cat. no. ab27278; Abcam), and mouse monoclonal anti-β-actin (1:5,000; cat. no. 3700; Cell Signaling Technology, Danvers, MA). Following washing with TBST, membranes were incubated with the appropriate horseradish peroxidase-conjugated secondary antibodies (Vector Laboratories, Burlingame, CA) for 1 h at room temperature. Membranes were subsequently washed and developed using ECL reagent (Thermo Fisher Scientific). Images were acquired using an iBright imaging system. Protein band intensities were quantified and normalized to the corresponding β-actin signal.

**Cell Proliferation, Colony Formation, and Transwell Migration Assays**

Cell proliferation was determined using an MTT assay as described previously (Chaudhary et al., 2025). Pituitary tumor cells were seeded in 96-well plates at a density of 3,000 cells per well in triplicate. Cell proliferation was assessed at 0, 24, 48, and 72 h. MTT solution (10 µL; 5

mg/mL in PBS) was added to each well, and plates were incubated for 3 h at 37°C. Subsequently, 100 µL of solubilization buffer containing 10% Triton X-100, 89% isopropanol, and 1% HCl was added to each well. Plates were incubated for an additional 15 min at 37°C, and absorbance was measured at 595 nm using a Multiskan FC plate reader (Thermo Fisher Scientific).

The colony formation assay was performed as described previously (Chaudhary et al., 2025). Pituitary tumor cells were seeded at 2,000 cells per well in six-well plates. After 14 days, colonies were washed with PBS, fixed with cold methanol for 10 min, and stained with 0.5% crystal violet in 25% methanol for 15 min. Plates were washed with water, air-dried overnight, and scanned. Colonies were counted using ImageJ software (National Institutes of Health).

Transwell migration assays were performed using 24 well plates containing 8-µm-pore inserts and Matrigel, as described previously (Chaudhary et al., 2025). Following the migration period, cells were stained with 0.1% crystal violet. Inserts were washed with distilled water and allowed to dry before microscopic imaging. Migrated cells were quantified using ImageJ software.

**Stable Overexpression of miR-129 or miR-182 in AF Rat Pituitary Tumor Cells**

The pCMV-miR expression vector (cat. no. PCMVMIR) and a pCMV-miR vector containing miR-129 (cat. no. SC400758) were purchased from OriGene (Rockville, MD). A pCMV-miR vector containing miR-182 was custom-generated by GenScript (Piscataway, NJ). Stable AF cell lines overexpressing miR-129 or miR-182, together with vector-control cells, were generated using standard transfection and selection procedures. Approximately 1 × 106 AF cells were seeded in 10-cm culture dishes and transfected with 4 µg of plasmid DNA using Lipofectamine 3000. Six hours after transfection, the medium was replaced with fresh culture medium. At 24 h after transfection, cells were selected with G418 (250 µg/mL), with fresh selection medium added

every 2–3 days. Selection was continued until all cells in the control plate had died. Vector-, miR-129-, and miR-182-transfected cells were passaged twice before use in subsequent experiments. MicroRNA was extracted from stable AF transfectants and control AF cells. TaqMan miRNA assays specific for miR-129 and miR-182 were used to confirm stable overexpression of the corresponding miRNAs.

**Xenograft Mouse Experiments**

NOD/SCID or NSG immunodeficient mice were used for xenograft studies as described previously (Chaudhary et al., 2025). Approximately $1 \times 10^6$ AF control cells, vector-control cells, miR-129-overexpressing cells, or miR-182-overexpressing cells were mixed with an equal volume of Matrigel (cat. no. CLS356234; Corning, Glendale, AZ) and injected subcutaneously into the right flank. Tumor dimensions were measured using Vernier calipers, and tumor volume was calculated using the formula: **$V = L \times W^2 \times 0.5$. Mean ± SEM tumor volume was calculated every other day until the experimental endpoint was reached. Following euthanasia, tumors were excised, weighed, and photographed to document differences in tumor morphology.

**Luciferase Reporter Assay**

The 3′UTRs of rat WNT-5A and VEGF-C were cloned into the psiCHECK-2 dual-luciferase reporter vector (Promega, Madison, WI), in which Renilla luciferase served as the experimental reporter and firefly luciferase served as the normalization control. HEK293 cells were seeded at a density of 25,000 cells per well in 96-well plates. Cells were transfected with 50 ng of reporter plasmid containing the target 3′UTR together with miR-129 mimic, miR-182 mimic, or negative-control mimic oligonucleotide at a final concentration of 50 nM using Lipofectamine 3000. After 48 h, Renilla and firefly luciferase activities were measured using the Dual-Glo Luciferase Assay System (Promega) with a BioTek Synergy HT plate reader. Eight samples were included in each

transfection group, and luciferase activity was measured in duplicate. Renilla luciferase activity was normalized to firefly luciferase activity.

### Statistical Analysis

Data are presented as mean ± SEM. Differences among treatment groups were analyzed using one-way **analysis** of variance (ANOVA) followed by the Newman–Keuls post hoc test. Statistical significance was defined as *, $p < 0.05$.

### Author contributions

OG and DKS conceived and designed the project. OG performed the experiment and analyzed the data, OG and DS wrote the paper.

### Competing interests

The author(s) declare no competing interests.

### Data availability

All the data are generated and presented in the figures and in the text of the manuscript.

## References


1. Jabbar S, Reuhl K, Sarkar DK. 2018 Prenatal alcohol exposure increases the susceptibility to develop aggressive prolactinomas in the pituitary gland. Sci Rep. 16;8(1):7720.
2. Ezzat S, Asa S.L. 2006 Mechanisms of disease: the pathogenesis of pituitary tumors. Nat. Clin. Pract. Endocrinol. Metab.; 2(4)220–230.

3. Yoshino A, Katayama Y, Ogino A, Watanabe T, Yachi K, Ohta T, Komine C, Yokoyama T, Fukushima T. 2007 Promoter hypermethylation profile of cell cycle regulator genes in pituitary adenomas. J Neurooncol.; 83(2):153-62.
4. Gangisetty O, Wynne O, Jabbar S, Nasello C, Sarkar DK. 2015 Fetal Alcohol Exposure Reduces Dopamine Receptor D2 and Increases Pituitary Weight and Prolactin Production via Epigenetic Mechanisms. PLoS One.;10(10):e0140699.
5. Chaudhary S, Das U, Jabbar S, Gangisetty O, Rousseau B, Hanft S, Sarkar DK. 2025 Developmental pluripotency-associated 4 increases aggressiveness of pituitary neuroendocrine tumors by enhancing cell stemness. Neuro Oncol. 12;27(1):123-139.
6. Calin GA, Sevignani C, Dumitru CD. et al., 2004. Human microRNA genes are frequently located at fragile sites and genomic regions involved in cancers. Proceedings of the National Academy of Sciences of the United States of America, vol. 101, no. 9, pp. 2999–3004,
7. Mohammadi-Yeganeh, S., Paryan, M., Arefian, E. *et al.* 2016. MicroRNA-340 inhibits the migration, invasion, and metastasis of breast cancer cells by targeting Wnt pathway. *Tumor Biol.* **37**, 8993–9000.
8. Liu D, Chen C, Cui M, Zhang H. 2021. miR-140-3p Inhibits Colorectal Cancer Progression and its Liver Metastasis by Targeting BCL9 and BCL2. Cancer Med. 10(10):3358–72.
9. Elnaggar GN, El-Hifnawi NM, Ismail A, Yahia M, Elshimy RAA. 2021. Micro RNA-148a Targets Bcl-2 in Patients With Non-Small Cell Lung Cancer. Asian Pacific J Cancer Prev. 22(6):1949–55.
10. Lamouille S, Xu J, Derynck R. 2014. Molecular mechanisms of epithelial-mesenchymal transition. Nat Rev Mol Cell Biol. 15(3):178-96.

11. Mao ZG, He DS, Zhou J, Yao B, Xiao WW, Chen CH, Zhu YH, Wang HJ. 2010. Differential expression of microRNAs in GH-secreting pituitary adenomas. Diagn Pathol.; 5:79.
12. Bottoni A, Zatelli MC, Ferracin M, Tagliati F, Piccin D, Vignali C, Calin GA, Negrini M, Croce CM, Degli Uberti EC. 2007. Identification of differentially expressed microRNAs by microarray: a possible role for microRNA genes in pituitary adenomas. J Cell Physiol. 210(2):370-7.
13. T. Palumbo, F. R. Faucz, M. Azevedo, P. Xekouki, D. Iliopoulos, and C. A. Stratakis 2013. Functional screen analysis reveals miR-26b and miR-128 as central regulators of pituitary somatomammotrophic tumor growth through activation of the PTEN-AKT pathway. Oncogene, 32 (13) : 1651–1659.
14. Grzywa TM, Klicka K, Rak B, Mehlich D, Garbicz F, Zieliński G, Maksymowicz M, Sajjad E, Włodarski PK. 2019. Lineage-dependent role of miR-410-3p as oncomiR in gonadotroph and corticotroph pituitary adenomas or tumor suppressor miR in somatotroph adenomas via MAPK, PTEN/AKT, and STAT3 signaling pathways. Endocrine. 65(3):646-655.
15. Renjie W, Haiqian L, 2015. MiR-132, miR-15a and miR-16 synergistically inhibit pituitary tumor cell proliferation, invasion and migration by targeting Sox5. Cancer Letters, 356( 2) 568-578.
16. Yu, Y. et al. 2015. Down-regulation of miR-129-5p via the Twist1-Snail feedback loop stimulates the epithelial-mesenchymal transition and is associated with poor prognosis in breast cancer. Oncotarget 6, 34423–34436.
17. Jiang, Z. et al. 2016. MiR-129-5p is down-regulated and involved in migration and invasion of gastric cancer cells by targeting interleukin-8. Neoplasma 63, 673–680.
18. Ma, N. et al. 2015. MicroRNA-129-5p inhibits hepatocellular carcinoma cell metastasis and invasion via targeting ETS1. Biochem. Biophys. Res. Commun. 461, 618–623.

19. Li J, Wang H, Ke H, Ni S. 2015. MiR-129 regulates MMP9 to control metastasis of non-small cell lung cancer. Tumour Biol. 36(8):5785-90.
20. Li Y, Zhang H, Gong H, Yuan Y, Li Y, Wang C, Li W, Zhang Z, Liu M, Liu H, Chen J. 2018. miR-182 suppresses invadopodia formation and metastasis in non-small cell lung cancer by targeting cortactin gene. J Exp Clin Cancer Res. 9;37(1):141.
21. Yan S, Wang H, Chen X, Liang C, Shang W, Wang L, Li J, Xu D. 2020. MiR-182-5p inhibits colon cancer tumorigenesis, angiogenesis, and lymphangiogenesis by directly downregulating VEGF-C. Cancer Lett. 488:18-26.
22. Ma YS, Shi BW, Lu HM, Xie PF, Xin R, Wu ZJ, Shi Y, Yin YZ, Hou LK, Jia CY, Wu W, Lv ZW, Yu F, Wang GR, Liu JB, Jiang GX, Fu D. 2021. MicroRNA-499 serves as a sensitizer for lung cancer cells to radiotherapy by inhibition of CK2α-mediated phosphorylation of p65. Mol Ther Oncolytics. 21:171-182.
23. Wang J, Li J, Chen L, Fan Z, Cheng J. 2020 MicroRNA-499 Suppresses the Growth of Hepatocellular Carcinoma by Downregulating Astrocyte Elevated Gene-1. Technol Cancer Res Treat. 19:1533033820920253.
24. Gangisetty O, Chaudhary S, Tarale P, Cabrera MA, Sarkar DK. 2023. miRNA-383 and miRNA-384 Suppress Proopiomelanocortin Gene Expression in the Hypothalamus: Effects of Early Life Ethanol Exposure. Neuroendocrinology. 113 (8) :844-858.
25. Zeng A, Yin J, Li Y, Li R, Wang Z, Zhou X, Jin X, Shen F, Yan W, You Y. 2018. miR-129-5p targets Wnt5a to block PKC/ERK/NF-κB and JNK pathways in glioblastoma. Cell Death Dis. 9 (3):394.
26. Zhang Y, Liu Z, Zhou M, Liu C. 2016. MicroRNA-129-5p inhibits vascular smooth muscle cell proliferation by targeting Wnt5a. Exp Ther Med. 12 (4) :2651-2656.
27. Li J, Wang H, Ke H, Ni S. 2015. MiR-129 regulates MMP9 to control metastasis of non-small cell lung cancer. Tumour Biol. 36(8):5785-90.

28. Z.G. Mao, D.S. He, J. Zhou, B. Yao, W.W. Xiao, C.H. Chen, et al., 2010. Differential expression of microRNAs in GH-secreting pituitary adenomas, Diagn. Pathol. 5:79.
29. Bottoni, M.C. Zatelli, M. Ferracin, F. Tagliati, D. Piccin, C. Vignali, et al., 2007. Identification of differentially expressed microRNAs by microarray: a possible role for microRNA genes in pituitary adenomas, J. Cell. Physiol. 210 : 370–377.
30. Pekarsky Y, Croce CM. 2015. Role of miR-15/16 in CLL. Cell Death Differ. 22(1):6-11.
31. Cimmino A, Calin GA, Fabbri M, Iorio MV, Ferracin M, Shimizu M, et al. 2005 miR-15 and miR-16 Induce Apoptosis by Targeting BCL2. Proc Natl Acad Sci USA 102(39):13944–9.
32. Gregory PA, Bert AG, Paterson EL, Barry SC, Tsykin A, Farshid G, et al. 2008. The miR-200 Family and miR-205 Regulate Epithelial to Mesenchymal Transition by Targeting ZEB1 and SIP1. Nat Cell Biol 10(5):593–601.
33. Title AC, Hong SJ, Pires ND, Hasenöhrl L, Godbersen S, Stokar-Regenscheit N, et al. 2018. Genetic Dissection of the miR-200–Zeb1 Axis Reveals its Importance in Tumor Differentiation and Invasion. Nat Commun. 9(1):4671.
34. Kappil M, Chen J. 2014. Environmental exposures in utero and microRNA. Curr Opin Pediatr. 26(2):243-51.
35. Wang LL, Zhang Z, Li Q, Yang R, Pei X, Xu Y, Wang J, Zhou SF, Li Y. 2009. Ethanol exposure induces differential microRNA and target gene expression and teratogenic effects which can be suppressed by folic acid supplementation. Hum Reprod. 24(3):562-79.
36. Sathyan P, Golden HB, Miranda RC. 2007. Competing interactions between micro-RNAs determine neural progenitor survival and proliferation after ethanol exposure: evidence from an ex vivo model of the fetal cerebral cortical neuroepithelium. J Neurosci. 27(32):8546-57.

37. Fan HD, Li YH, Yuan FQ, Lu LH, Liu J, Feng WK, Zhang HG, Chen SY, 2022. Up-regulation of microRNA-34a mediates ethanol-induced impairment of neural crest cell migration in vitro and in zebrafish embryos through modulating epithelial- mesenchymal transition by targeting Snail1. Toxicol. Lett. 358: 17–26.
38. Ambros V. 2004. The functions of animal microRNAs. Nature. 431(7006):350-5.
39. Bartel DP. 2004. MicroRNAs: genomics, biogenesis, mechanism, and function. Cell. 116(2):281-97.
40. Forsyth CB, Tang Y, Shaikh M, Zhang L, Keshavarzian A. 2010. Alcohol stimulates activation of Snail, epidermal growth factor receptor signaling, and biomarkers of epithelial-mesenchymal transition in colon and breast cancer cells. Alcohol Clin Exp Res. 34(1):19-31.
41. Welsch T, Kleeff J, Seitz HK, Büchler P, Friess H, Büchler MW. 2016. Update on pancreatic cancer and alcohol-associated risk. J Gastroenterol Hepatol. 21 Suppl 3:S69-75.
42. Papa NP, MacInnis RJ, Jayasekara H, English DR, Bolton D, Davis ID, Lawrentschuk N, Millar JL, Pedersen J, Severi G, Southey MC, Hopper JL, Giles GG. 2017 Total and beverage-specific alcohol intake and the risk of aggressive prostate cancer: a case-control study. Prostate Cancer Prostatic Dis. 20(3):305-310.
43. Kornet M, Goosen C, Thyssen JH, Van Ree JM. 1991 Endocrine profile during acquisition of free choice alcohol drinking in rhesus monkeys: treatment with desglycinamide-(Arg 8)-vasopressin. Alcohol 27:403-410.
44. De A, Boyadjieva N, Oomizu S, Sarkar DK. 2002 Ethanol induces hyperprolactinemia by increasing prolactin release and lactotrope growth in female rats. Alcohol Clin Exp Res. 2002 26(9):1420-9.

45. Gangisetty O, Jabbar S, Wynne O, Sarkar DK. 2017. MicroRNA-9 regulates fetal alcohol-induced changes in D2 receptor to promote prolactin production. J Endocrinol. 235(1):1-14.
46. Yu Y, Zhao Y, Sun XH, Ge J, Zhang B, Wang X, Cao XC. 2015 Down-regulation of miR-129-5p via the Twist1-Snail feedback loop stimulates the epithelial-mesenchymal transition and is associated with poor prognosis in breast cancer. Oncotarget 6:34423-34436.
47. Ma Z, Cai H, Zhang Y, Chang L, Cui Y. 2017. MiR-129-5p inhibits non-small cell lung cancer cell stemness and chemoresistance through targeting DLK1. Biochem Biophys Res Commun. 490(2):309-316.
48. Liu F, Zhao H, Gong L, Yao L, Li Y, Zhang W. 2018. MicroRNA-129-3p functions as a tumor suppressor in serous ovarian cancer by targeting BZW1. Int J Clin Exp Pathol. 11(12):5901-5908.
49. Dossing KB, Binderup T, Kaczkowski B, Jacobsen A, Rossing M, Winther O, Federspiel B, Knigge U, Kjær A, Friis-Hansen L. 2014 Down-Regulation of miR-129-5p and the let-7 Family in Neuroendocrine Tumors and Metastases Leads to Up-Regulation of Their Targets Egr1, G3bp1, Hmga2 and Bach1. Genes (Basel). 6(1):1-21.
50. Skaftnesmo KO, Prestegarden L, Micklem DR, Lorens JB. 2007 MicroRNAs in tumori-genesis. Curr Pharm Biotechnol. 8(6):320–5.
51. Chang H, Liu Y-H, Wang L-L, Wang J, Zhao Z-H, Qu J-F, Wang S-F. 2018 MiR-182 promotes cell proliferation by suppressing FBXW7 and FBXW11 in non-small cell lung cancer. Am J translational Res. 10 (4) :1131.
52. Hu J, Lv G, Zhou S, Zhou Y, Nie B, Duan H, Zhang Y, Yuan X. 2015. The downregulation of MiR-182 is associated with the growth and invasion of osteosarcoma cells through the regulation of TIAM1 expression. PLoS ONE. 10 (5) : e0121175.

53. Zhang Z-F, Wang Y-J, Fan S-H, Du S-X, Li X-D, Wu D-M, Lu J, Zheng Y-L. 2017 MicroRNA-182 downregulates Wnt/β-catenin signaling, inhibits proliferation, and promotes apoptosis in human osteosarcoma cells by targeting HOXA9. *Oncotarget* 8(60):101345.

**Figure Legend:**

**Figure 1. PAE promotes tumorigenic features and alters miRNA expression profile of rat pituitary tumor cells.** A. Morphology of cells isolated from AD and AF rat pituitary tumors B. Cell proliferation of AD and AF cells assessed by MTT assay (Data are mean ± SEM of n=8 per group and were analyzed using unpaired t- test. Significance at **p<0.01 between AF and AD cells). C. Colony formation of AD and AF cells. D. Cell migration of AD and AF cells. E. Tilda array analysis of miRNA profile of AF cells over AD are represented as volcano plot. Log2 fold change on X-axis. -Log2 (p-value) on Y axis. Differentially expressed miRNAs were determined with threshold of 10-fold change with p<0.05. F. Heat map representation of differentially expressed miRNA of AD and AF rat pituitary tumor cells.

**Figure 2. PAE reduces miR-129, 182 and 499 in rat pituitary tumor cells and tissue.** Taqman assay of miR-129 (A), miR-182 (B), miR-499 (C) in AD and AF cells. Expression levels of miR-129 (D), miR-182 (E), miR-499 (F) in AD, PF, and AF rat pituitary tumor tissue. U6 snRNA is used as negative control. Data are mean ± SEM of n=6 animals per group and were analyzed using one way ANOVA with Newman Keuls post hoc test. Significance at **p<0.01, ***p<0.001 between AF and AD or PF controls.

**Figure 3. Mir-129 overexpression reduced the tumorigenic characteristic features of AF rat pituitary tumor cells.** AF rat pituitary cells were transfected with miR-129 or negative control mimic oligo, mock control and harvested cells after 24h of transfection were analyzed for miR-129 expression and tumorigenic features. miR-129 expression (A), Cell proliferation (B), Colony formation (C), Cell migration (E). The quantification of colony formation was analyzed by measuring the absorbance of color produced with the colonies at 540nm (D). Cell migration rate was represented as percentage (F). Data are mean ± SEM of n=6 samples per group and were analyzed using one way ANOVA with Newman Keuls post hoc test. Significance at *p<0.05, **p<0.01, ***p<0.001 between miR-129 mimic verses negative control mimic or mock control.

**Figure 4. Mir-182 overexpression reduced the tumorigenic characteristic features of AF rat pituitary tumor cells.** AF rat pituitary cells were transfected with miR-182 or negative control mimic oligo, mock control and harvested cells after 24h of transfection were analyzed for miR-182 expression and tumorigenic features. Mir-182 expression (A), Cell proliferation (B), Colony formation (C), Cell migration (E). The quantification of colony formation was analyzed by measuring the absorbance of color produced with the colonies at 540nm (D). Cell migration rate was represented as percentage (F). Data are mean ± SEM of n=6 samples per group and were analyzed using one way ANOVA with Newman Keuls post hoc test. Significance at ***p<0.001 between miR-182 mimic verses negative control mimic or mock control.

**Figure 5. Mir-499 overexpression did not alter the tumorigenic characteristic features of AF rat pituitary tumor cells.** AF rat pituitary cells were transfected with miR-

499 or negative control mimic oligo, mock control and harvested cells after 24h of transfection were analyzed for miR-499 expression and tumorigenic features. Mir-499 expression (A), Cell proliferation (B), Colony formation (C), Cell migration (E). The quantification of colony formation was analyzed by measuring the absorbance of color produced with the colonies at 540nm (D). Cell migration rate was represented as percentage (F). Data are mean ± SEM of n=6 samples per group and were analyzed using one way ANOVA with Newman Keuls post hoc test. Significance at ***p<0.05 between miR-499 mimic verses negative control mimic or mock control.

**Figure 6. Stable over expression of miR-129, miR-182 reduced cell proliferation.** A. Schematic representation of pCMV miR vector with miR-129 or miR-182 sequences cloned. Plasmid DNA were transfected in AF rat pituitary cells and stable transfectants were generated with neomycin resistant marker. The expression of miR-129 (B), miR-182 (C) were measured by Taqman real time PCR. Cell proliferation of miR-129 stable AF cells (D), miR-182 stable AF cells (E) along with vector or mock controls were determined by MTT assay. Data are mean ± SEM of n=6 samples per group and were analyzed using one way ANOVA with Newman Keuls post hoc test. Significance at **p<0.01, ***p<0.001 between miR-499 mimic verses negative control mimic or mock control.

**Figure 7. Xenograft mouse model of AF-miR129 or AF-182 reduced tumor size, volume and wight.** AF control, AF-Vector, AF-miR-129, AF-182 cells were injected in NOD/SCID mice and tumors produced were examined (A), Tumor excised from each represented group was presented (B). Tumor volume was calculated with measured tumor diameter at different time periods of each mouse group is given as line diagram (C) Tumor weight of AF-control, vector, miR-129, miR-182 is represented in bar diagram (D). Data are

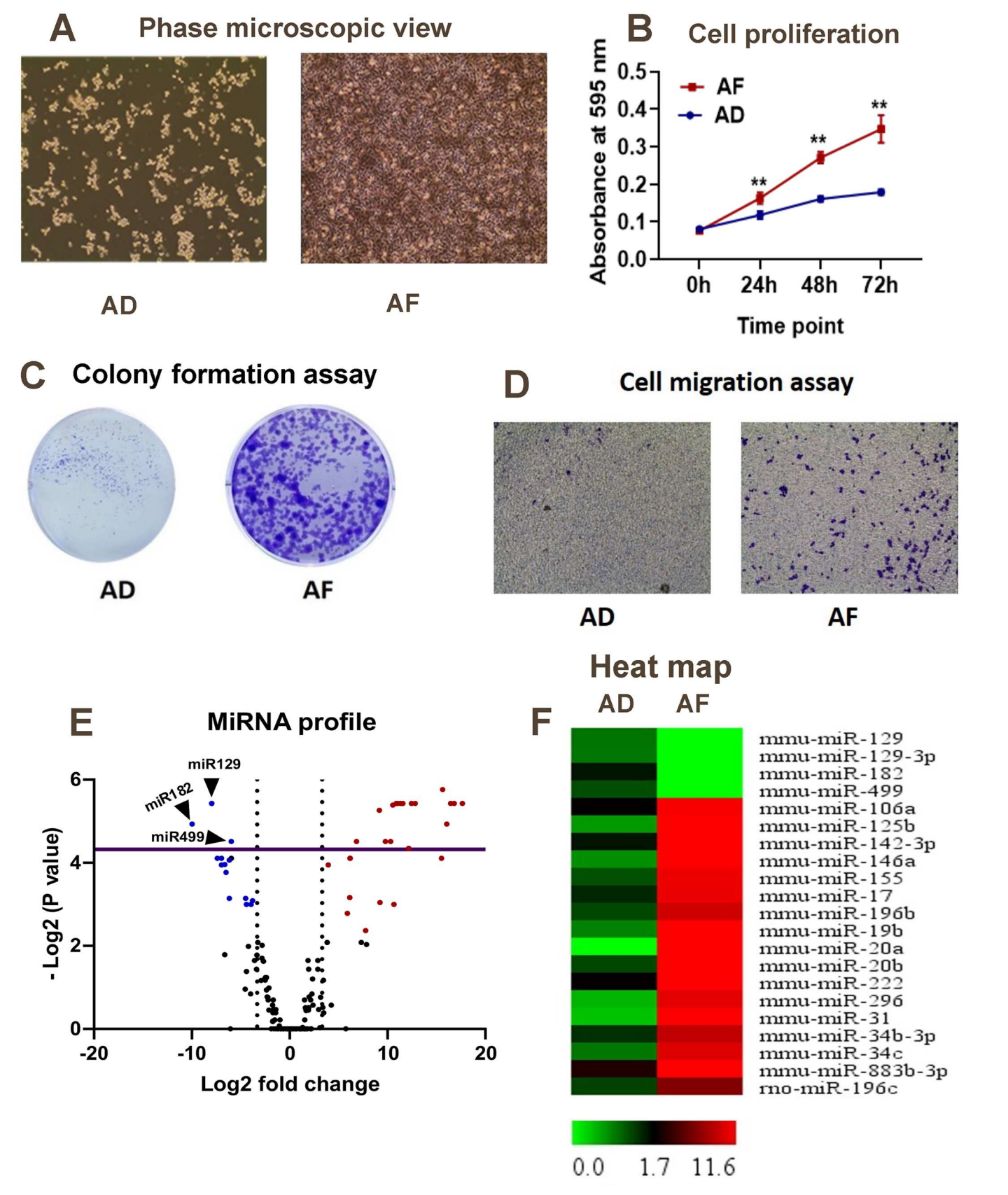
mean ± SEM of n=6 samples per group and were analyzed using one way ANOVA with Newman Keuls post hoc test. Significance at **p<0.01, ***p<0.001 between miR-129 or miR-182 AF cells verses Vector and control AF cells.

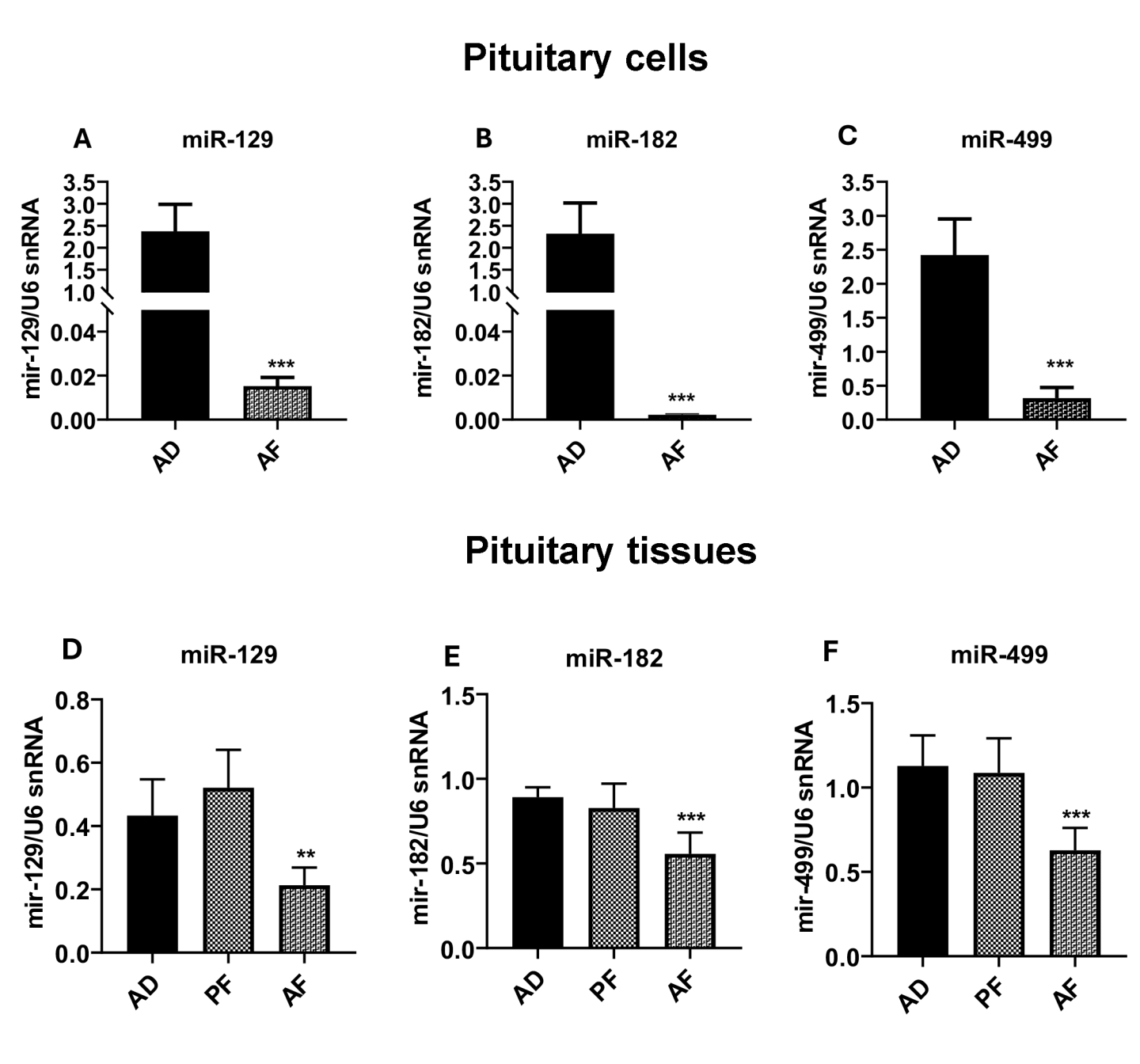
**Figure 8. Mir-129 over expression reduced Sox-2, Wnt-5A and MMP-19 expression in AF rat pituitary cells.** AF rat pituitary cells were transfected with miR-129 or negative control mimic oligo, mock control and harvested cells after 24h of transfection were analyzed for target gene, protein expression. A. Sox2 mRNA, B. MMP19 mRNA, C. BCL2 mRNA, D. Wnt-5A mRNA, E. KLF7 mRNA, F. Wnt-5A protein G. MMP19 protein. Gene expression was normalized with GAPDH, protein expression was normalized with β-actin. Representative blots for target protein and β-actin were shown in top panel, quantification data was represented as histogram in bottom panel. Data are mean ± SEM of n=6 samples per group and were analyzed using one way ANOVA with Newman Keuls post hoc test. Significance at **p<0.01, ***p<0.001 between miR-129 mimic verses NC mimic or control.

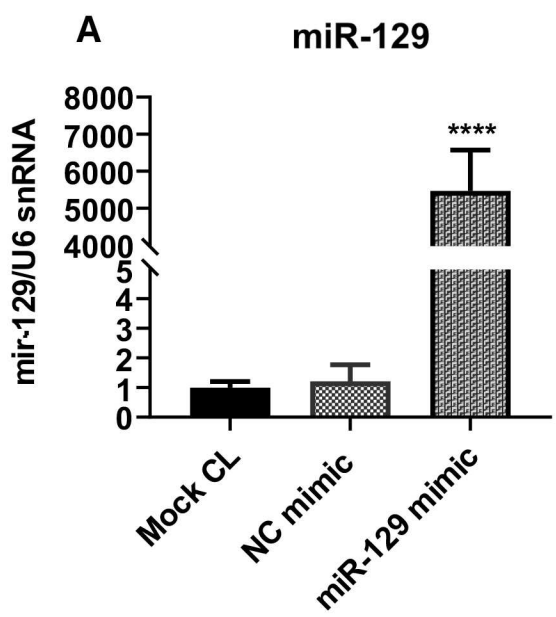
**Figure 9. Mir-182 over expression reduced VEGF-C, VEGF-R3 expression in AF rat pituitary cells.** AF rat pituitary cells were transfected with miR-182 or negative control mimic oligo, mock control and harvested cells after 24h of transfection were analyzed for target gene, protein expression. A. Sox2 mRNA, B. MMP16 mRNA, C. BCL2 mRNA, D. Wnt-5A mRNA, E. KLF7 mRNA, F. VEGF-A mRNA, G. VEGF-C mRNA, H. VEGF-D mRNA, I. VEGF-R3 mRNA, J. VEGF-C protein, K. VEGF-R3 protein. Gene expression was normalized with GAPDH, protein expression was normalized with β-actin. Representative blots for target protein and β-actin were shown in top panel, quantification data was represented as histogram in bottom panel. Data are mean ± SEM of n=6 samples per group and were analyzed using one way ANOVA with

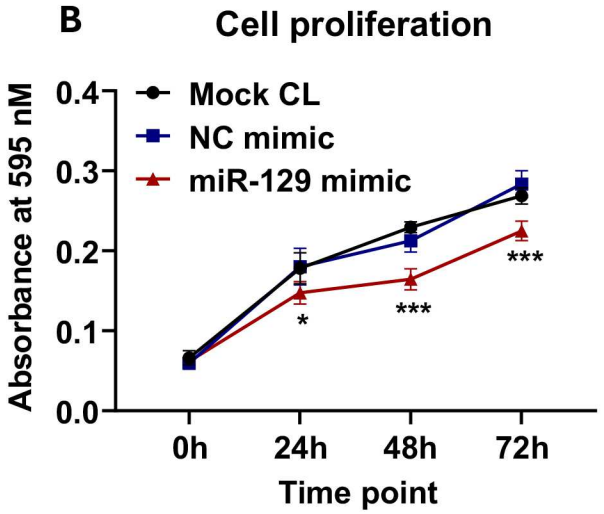
Newman Keuls post hoc test. Significance at **p<0.01, ***p<0.001 between miR-182 mimic verses NC mimic or control.

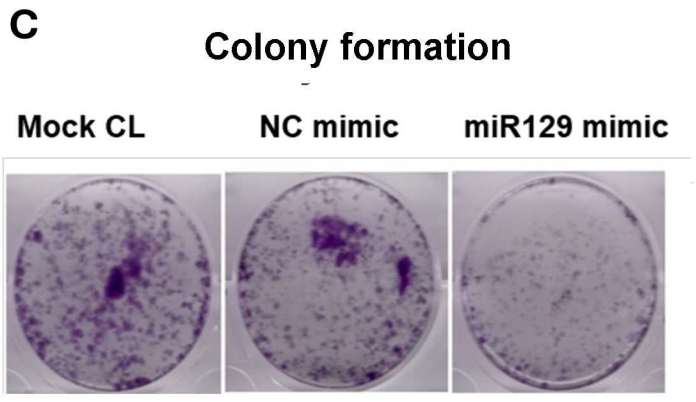
**Figure 10. Mir-129 target Wnt-5A 3'UTR, miR-182 target VEGF-C 3'UTR to repress its expression.** A. Schematic representation of Wnt-5A or VEGF-C 3' UTR sequences cloned down stream of renilla luciferase reporter in a reporter vector. Firefly luciferase is used as normalization control. HEK293 cells were transfected with a reporter plasmid carrying Wnt-5A or VEGF-C 3'UTR alone or plasmid along with negative control mimic or miR-129 or miR-182 mimic oligo and measured the luciferase activity after 48h of transfection. B. Wnt-5A 3'UTR sequence carrying miR-129-5P binding site aligned with miR-129-5P sequence (top panel), luciferase activity normalized (bottom panel). C. VEGF-C 3'UTR sequence carrying miR-182-5P binding site aligned with miR-182-5P sequence (top panel), luciferase activity normalized (bottom panel). Data are mean $\pm$ SEM of n=12 samples per group and were analyzed using one way ANOVA with Newman Keuls post hoc test. Significance at ***p<0.001 between miRNA mimic verses NC mimic oligo. or control.

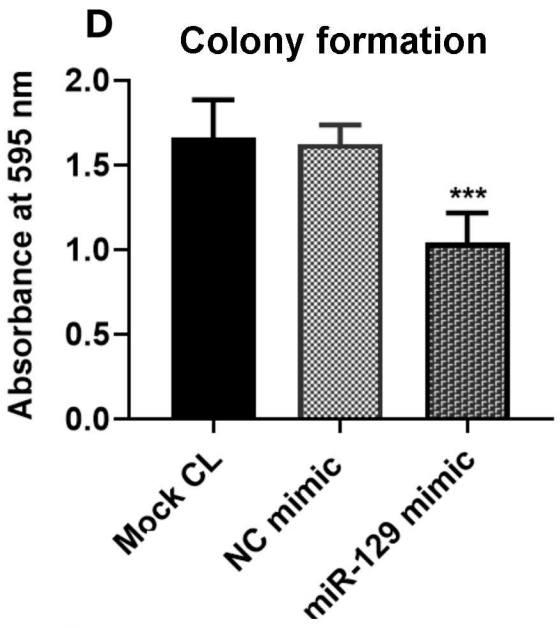

A
Phase microscopic view
AD
AF
B
Cell proliferation
Absorbance at 595 nm
0.5
0.4
0.3
0.2
0.1
0.0
AF
AD
**
**
**
0h
24h
48h
72h
Time point
C
Colony formation assay
AD
AF
D
Cell migration assay
AD
AF
E
MiRNA profile
miR129
miR182
miR499
6
4
2
0
-Log2 (P value)
-20
-10
0
10
20
Log2 fold change
F
Heat map
AD
AF
mmu-miR-129
mmu-miR-129-3p
mmu-miR-182
mmu-miR-499
mmu-miR-106a
mmu-miR-125b
mmu-miR-142-3p
mmu-miR-146a
mmu-miR-155
mmu-miR-17
mmu-miR-196b
mmu-miR-19b
mmu-miR-20a
mmu-miR-20b
mmu-miR-222
mmu-miR-296
mmu-miR-31
mmu-miR-34b-3p
mmu-miR-34c
mmu-miR-883b-3p
rno-miR-196c
0.0
1.7
11.6

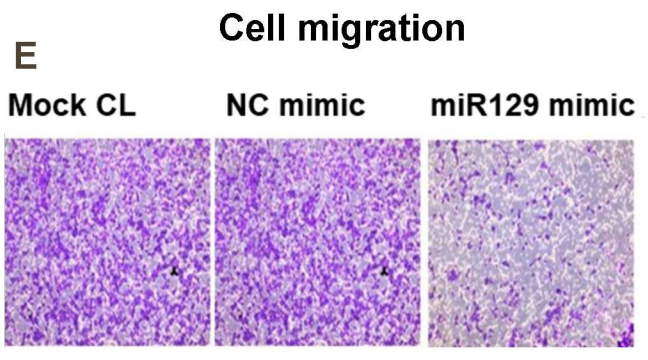

Pituitary cells
A
miR-129
mir-129/U6 snRNA
3.5
3.0
2.5
2.0
1.5
1.0
0.04
0.02
0.00
***
AD
AF
B
miR-182
mir-182/U6 snRNA
3.5
3.0
2.5
2.0
1.5
1.0
0.04
0.02
0.00
***
AD
AF
C
miR-499
mir-499/U6 snRNA
3.5
3.0
2.5
2.0
1.5
1.0
0.5
0.0
***
AD
AF
Pituitary tissues
D
miR-129
mir-129/U6 snRNA
0.8
0.6
0.4
0.2
0.0
**
AD
PF
AF
E
miR-182
mir-182/U6 snRNA
1.5
1.0
0.5
0.0
***
AD
PF
AF
F
miR-499
mir-499/U6 snRNA
1.5
1.0
0.5
0.0
***
AD
PF
AF

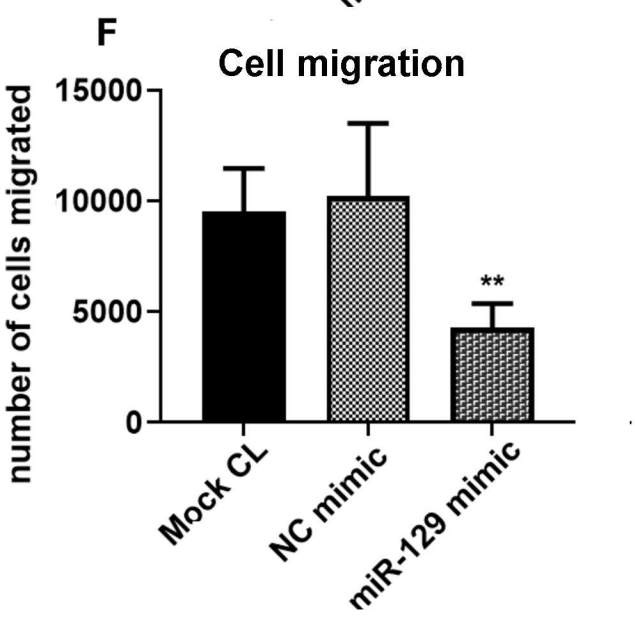

A
miR-129
mir-129/U6 snRNA
8000
7000
6000
5000
4000
5
4
3
2
1
0
****
Mock CL
NC mimic
miR-129 mimic

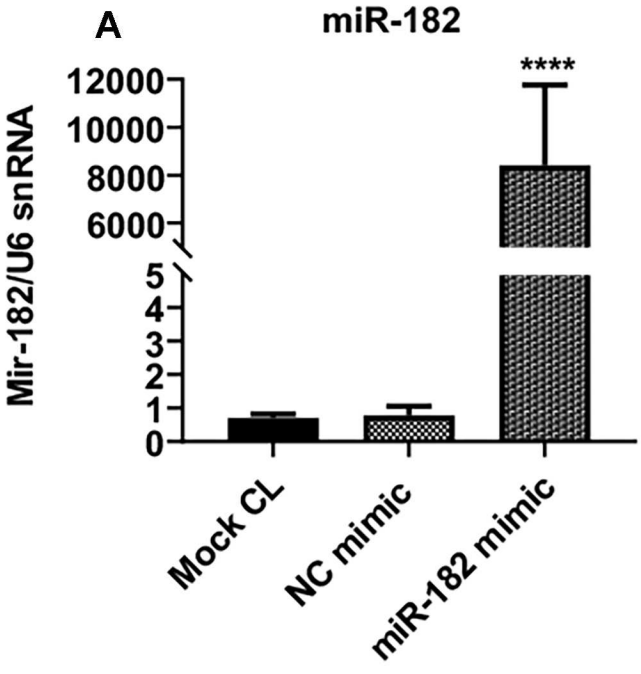

B
Cell proliferation
Absorbance at 595 nM
0.4
0.3
0.2
0.1
0.0
Mock CL
NC mimic
miR-129 mimic
*
***
***
0h
24h
48h
72h
Time point

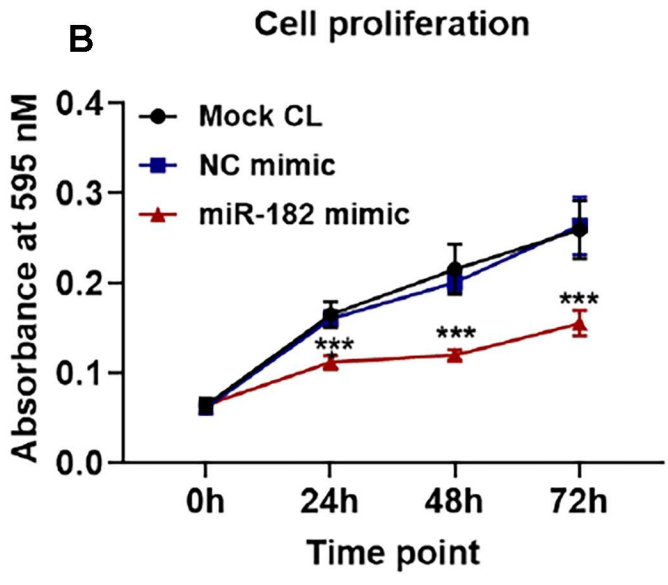

C
Colony formation
Mock CL
NC mimic
miR129 mimic

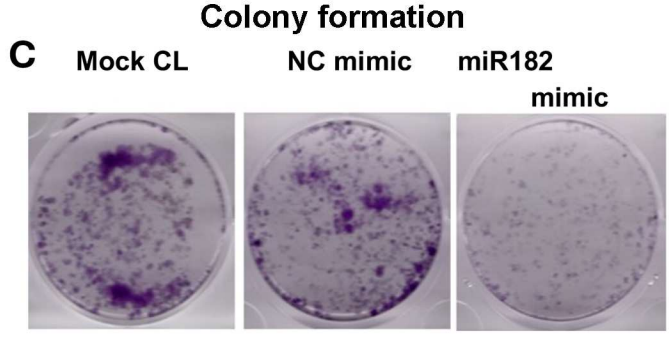

D
Colony formation
Absorbance at 595 nm
2.0
1.5
1.0
0.5
0.0
***
Mock CL
NC mimic
miR-129 mimic

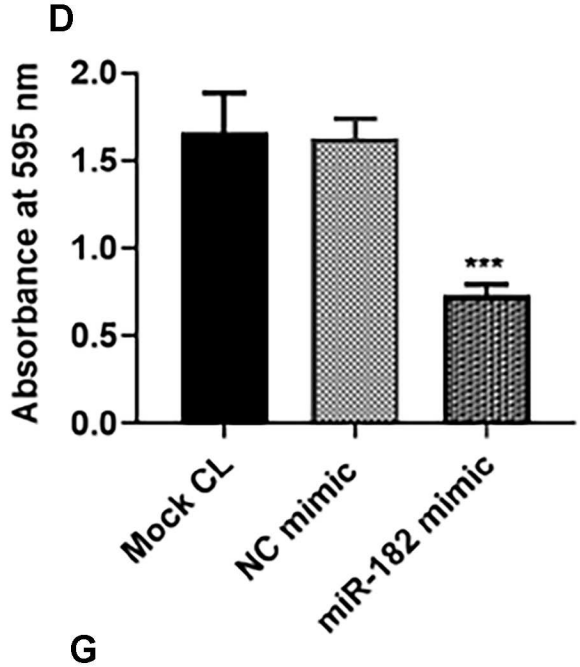

E
Cell migration
Mock CL
NC mimic
miR129 mimic

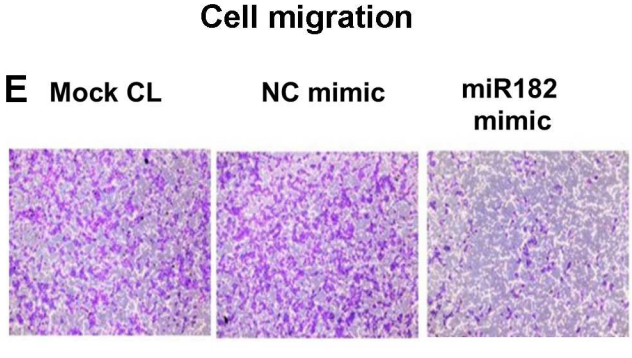

F
Cell migration
number of cells migrated
15000
10000
5000
0
**
Mock CL
NC mimic
miR-129 mimic

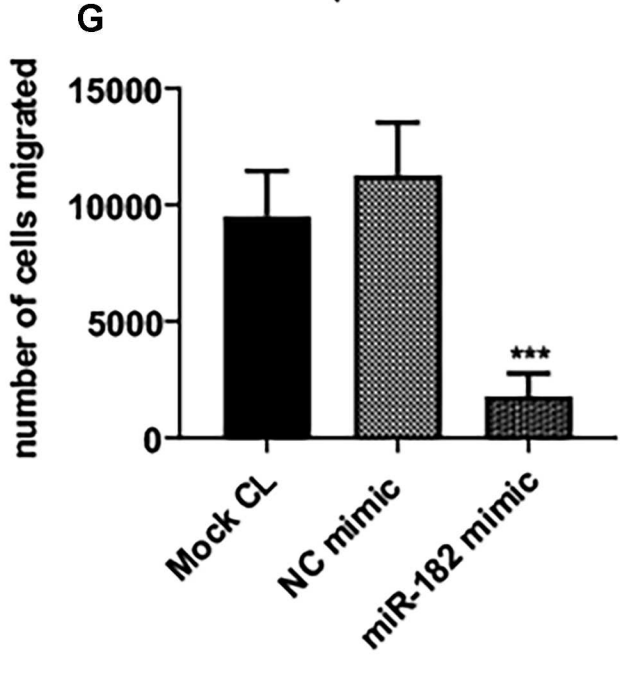

A
miR-182
Mir-182/U6 snRNA
12000
10000
8000
6000
5
4
3
2
1
0
****
Mock CL
NC mimic
miR-182 mimic

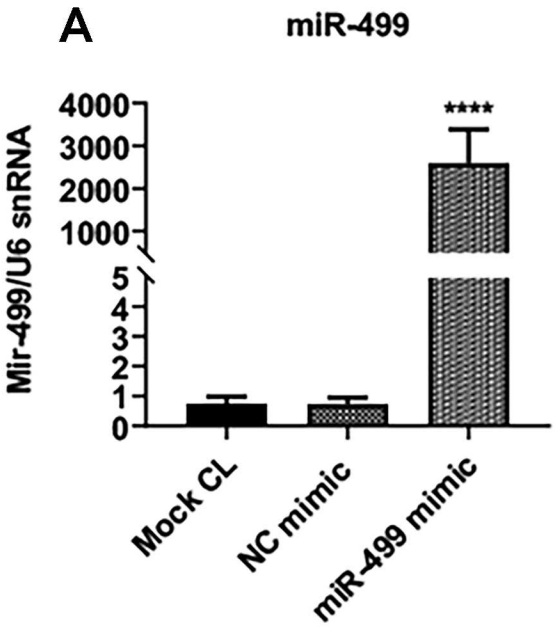

B
Cell proliferation
Absorbance at 595 nM
0.4
0.3
0.2
0.1
0.0
Mock CL
NC mimic
miR-182 mimic
***
***
***
0h
24h
48h
72h
Time point

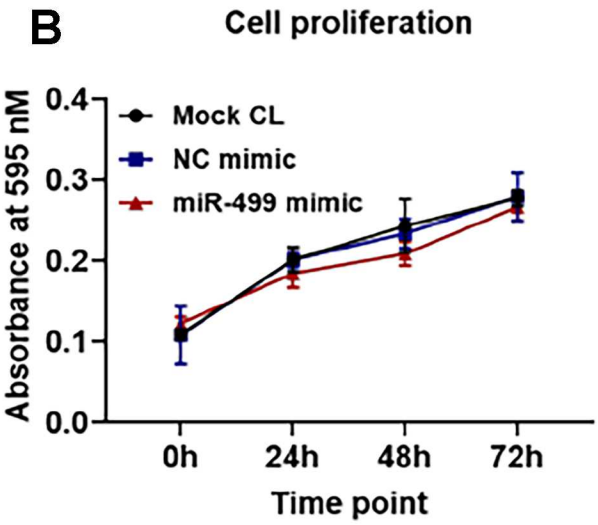

Colony formation
C
Mock CL
NC mimic
miR182 mimic

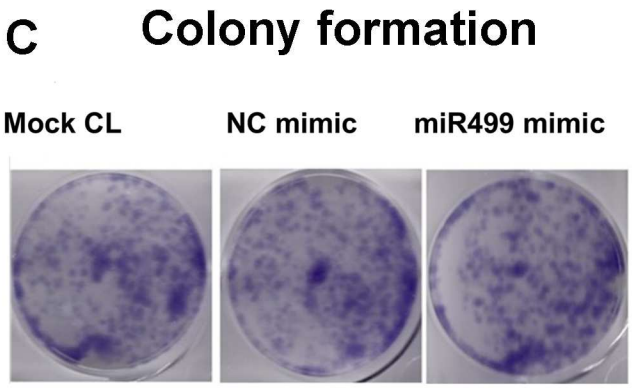

D
Absorbance at 595 nm
2.0
1.5
1.0
0.5
0.0
***
Mock CL
NC mimic
miR-182 mimic

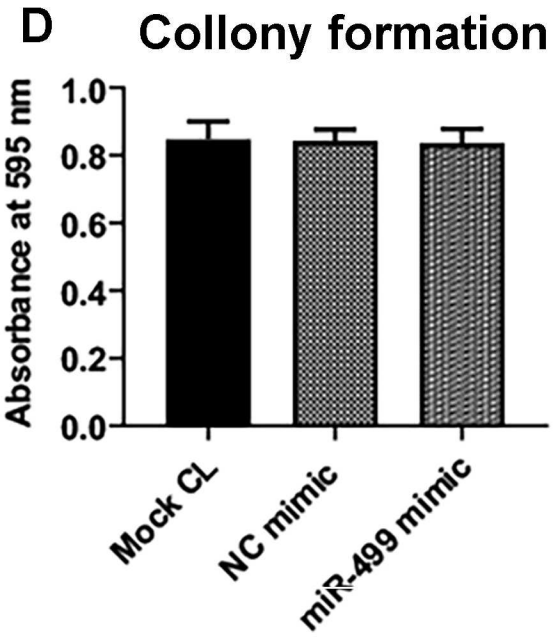

Cell migration
E
Mock CL
NC mimic
miR182 mimic

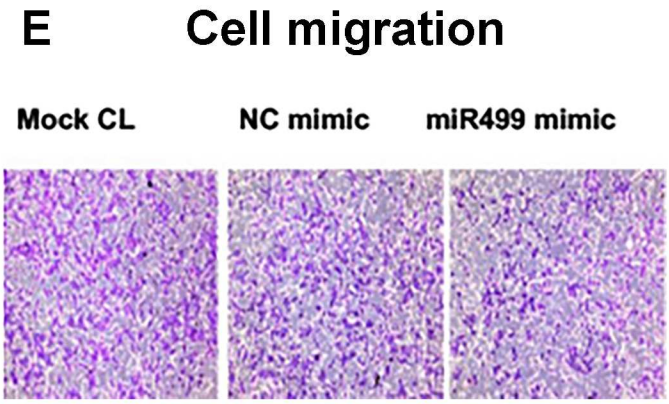

G
number of cells migrated
15000
10000
5000
0
***
Mock CL
NC mimic
miR-182 mimic

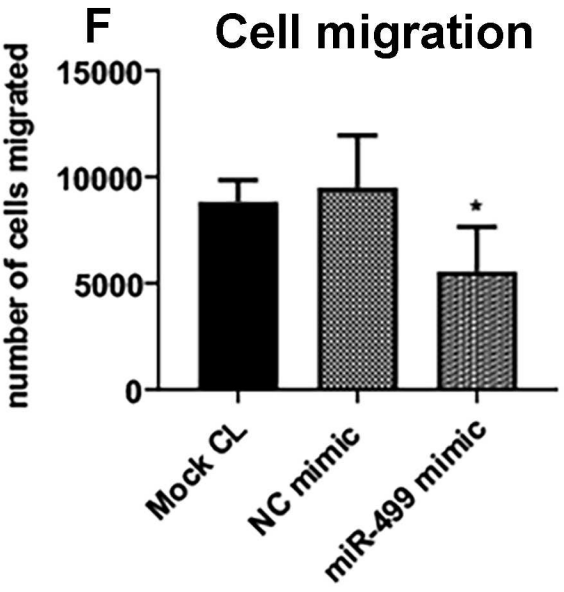

A
miR-499
Mir-499/U6 snRNA
4000
3000
2000
1000
5
4
3
2
1
0
****
Mock CL
NC mimic
miR-499 mimic

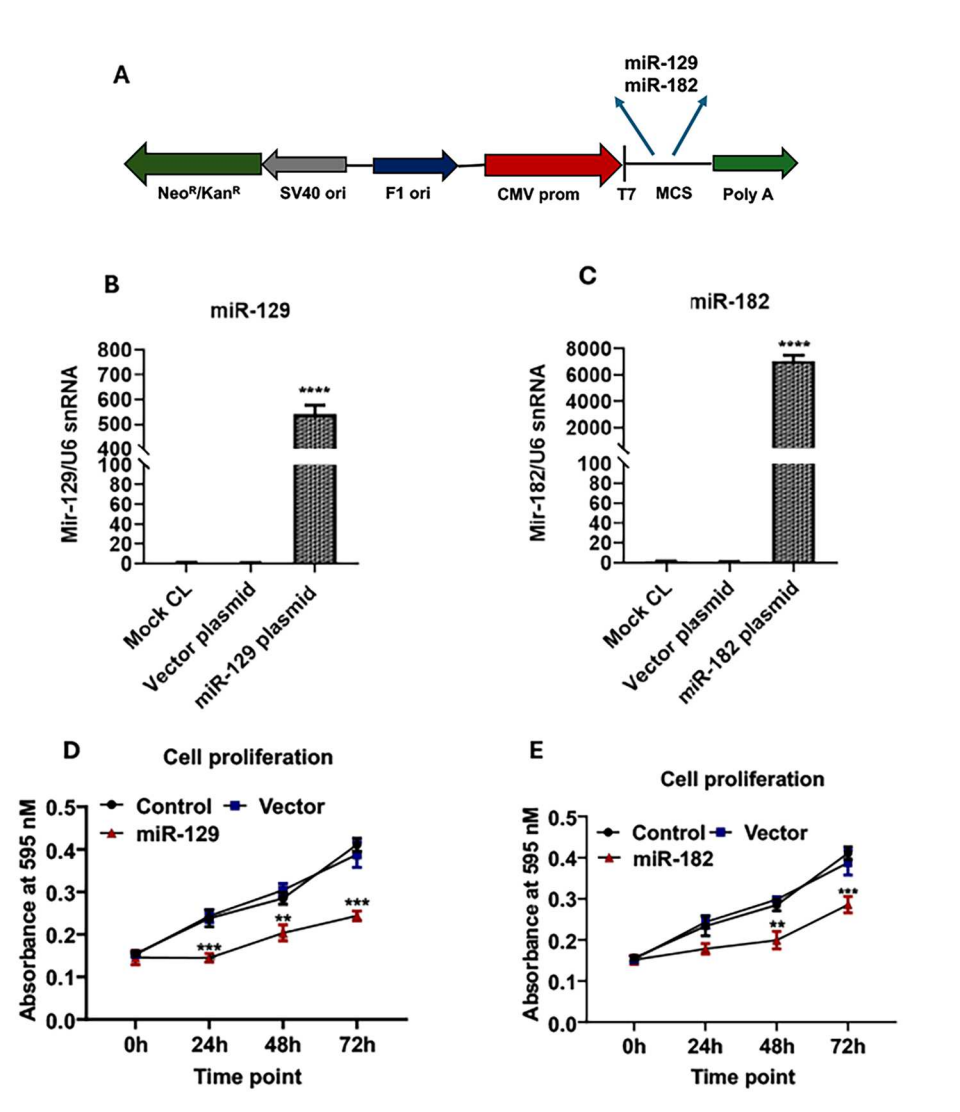

B
Cell proliferation
Absorbance at 595 nM
0.4
0.3
0.2
0.1
0.0
Mock CL
NC mimic
miR-499 mimic
0h
24h
48h
72h
Time point

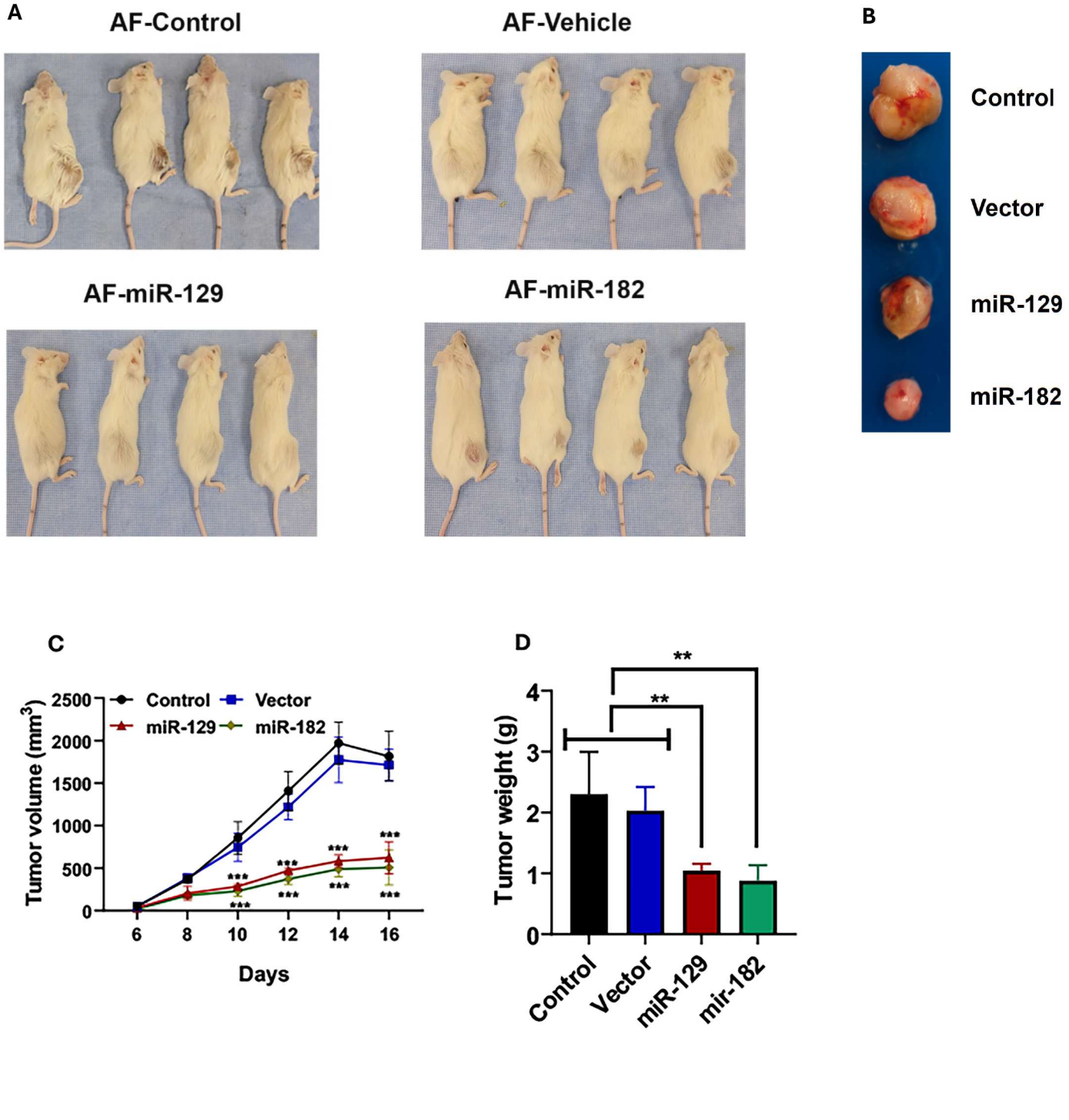

C
Colony formation
Mock CL
NC mimic
miR499 mimic

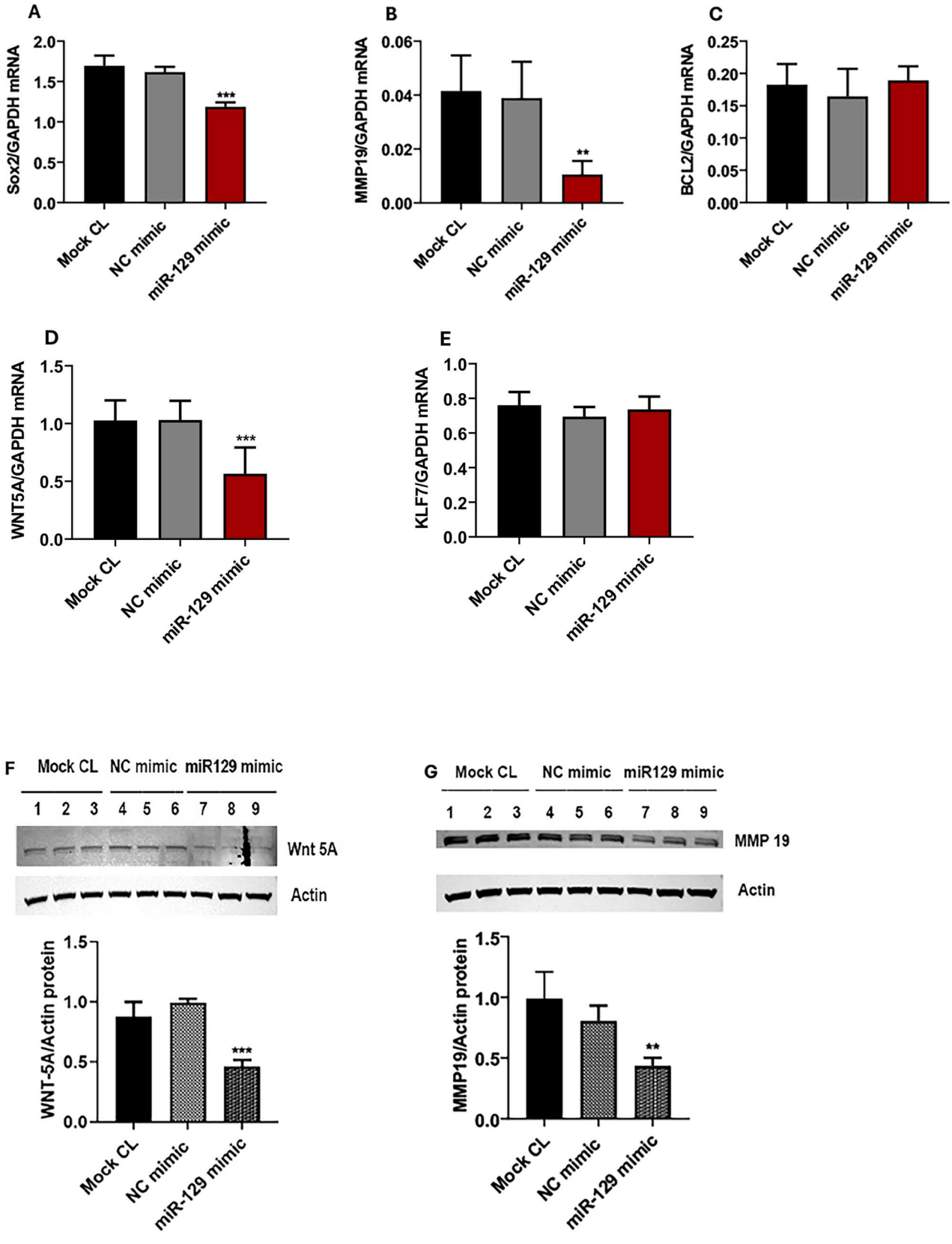

D
Collony formation
Absorbance at 595 nm
1.0
0.8
0.6
0.4
0.2
0.0
Mock CL
NC mimic
miR-499 mimic

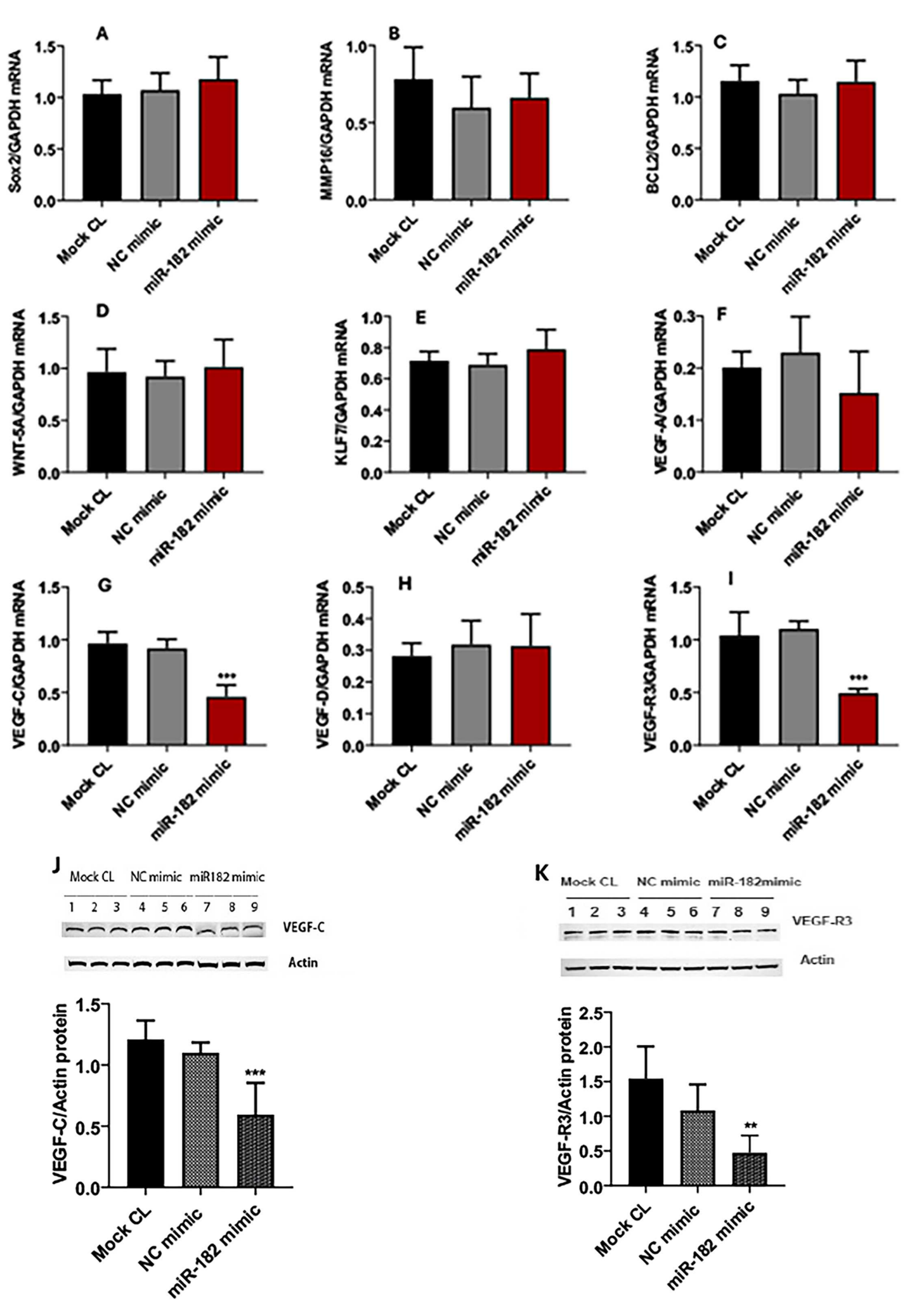

E
Cell migration
Mock CL
NC mimic
miR499 mimic

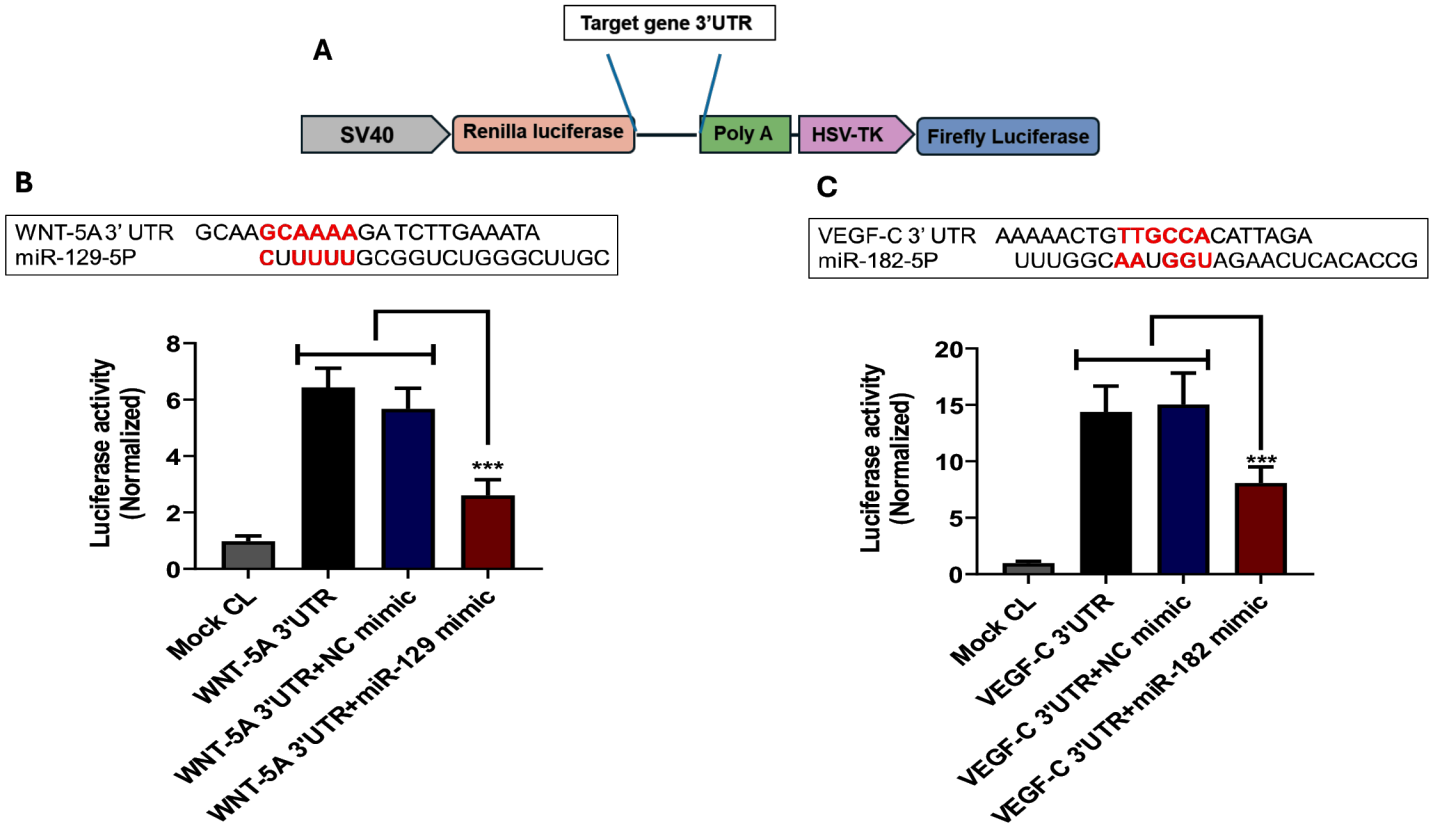

F
Cell migration
number of cells migrated
15000
10000
5000
0
*
Mock CL
NC mimic
miR-499 mimic


A
miR-129
miR-182
Neo^R/Kan^R
SV40 ori
F1 ori
CMV prom
T7
MCS
Poly A
B
miR-129
Mir-129/U6 snRNA
800
700
600
500
400
100
80
60
40
20
0
****
Mock CL
Vector plasmid
miR-129 plasmid
C
miR-182
Mir-182/U6 snRNA
8000
6000
4000
2000
100
80
60
40
20
0
****
Mock CL
Vector plasmid
miR-182 plasmid
D
Cell proliferation
Absorbance at 595 nM
0.5
0.4
0.3
0.2
0.1
0.0
Control
Vector
miR-129
***
**
***
0h
24h
48h
72h
Time point
E
Cell proliferation
Absorbance at 595 nM
0.5
0.4
0.3
0.2
0.1
0.0
Control
Vector
miR-182
**
***
0h
24h
48h
72h
Time point


A
AF-Control
AF-Vehicle
AF-miR-129
AF-miR-182
B
Control
Vector
miR-129
miR-182
C
Control
Vector
miR-129
miR-182
Tumor volume (mm3)
2500
2000
1500
1000
500
0
6
8
10
12
14
16
Days
***
D
**
**
Tumor weight (g)
4
3
2
1
0
Control
Vector
miR-129
mir-182


A
Sox2/GAPDH mRNA
2.0
1.5
1.0
0.5
0.0
***
Mock CL
NC mimic
miR-129 mimic
B
MMP19/GAPDH mRNA
0.06
0.04
0.02
0.00
**
Mock CL
NC mimic
miR-129 mimic
C
BCL2/GAPDH mRNA
0.25
0.20
0.15
0.10
0.05
0.00
Mock CL
NC mimic
miR-129 mimic
D
WNT5A/GAPDH mRNA
1.5
1.0
0.5
0.0
***
Mock CL
NC mimic
miR-129 mimic
E
KLF7/GAPDH mRNA
1.0
0.8
0.6
0.4
0.2
0.0
Mock CL
NC mimic
miR-129 mimic
F
Mock CL
NC mimic
miR129 mimic
1 2 3 4 5 6 7 8 9
Wnt 5A
Actin
WNT-5A/Actin protein
1.5
1.0
0.5
0.0
***
Mock CL
NC mimic
miR-129 mimic
G
Mock CL
NC mimic
miR129 mimic
1 2 3 4 5 6 7 8 9
MMP 19
Actin
MMP19/Actin protein
1.5
1.0
0.5
0.0
**
Mock CL
NC mimic
miR-129 mimic


A
Sox2/GAPDH mRNA
1.5
1.0
0.5
0.0
Mock CL
NC mimic
miR-182 mimic
B
MMP16/GAPDH mRNA
1.0
0.5
0.0
Mock CL
NC mimic
miR-182 mimic
C
BCL2/GAPDH mRNA
1.5
1.0
0.5
0.0
Mock CL
NC mimic
miR-182 mimic
D
WNT-5A/GAPDH mRNA
1.5
1.0
0.5
0.0
Mock CL
NC mimic
miR-182 mimic
E
KLF7/GAPDH mRNA
1.0
0.8
0.6
0.4
0.2
0.0
Mock CL
NC mimic
miR-182 mimic
F
VEGF-A/GAPDH mRNA
0.3
0.2
0.1
0.0
Mock CL
NC mimic
miR-182 mimic
G
VEGF-C/GAPDH mRNA
1.5
1.0
0.5
0.0
***
Mock CL
NC mimic
miR-182 mimic
H
VEGF-D/GAPDH mRNA
0.5
0.4
0.3
0.2
0.1
0.0
Mock CL
NC mimic
miR-182 mimic
I
VEGF-R3/GAPDH mRNA
1.5
1.0
0.5
0.0
***
Mock CL
NC mimic
miR-182 mimic
J
Mock CL
NC mimic
miR182 mimic
1 2 3 4 5 6 7 8 9
VEGF-C
Actin
VEGF-C/Actin protein
1.5
1.0
0.5
0.0
***
Mock CL
NC mimic
miR-182 mimic
K
Mock CL
NC mimic
miR-182mimic
1 2 3 4 5 6 7 8 9
VEGF-R3
Actin
VEGF-R3/Actin protein
2.5
2.0
1.5
1.0
0.5
0.0
**
Mock CL
NC mimic
miR-182 mimic


A
Target gene 3'UTR
SV40
Renilla luciferase
Poly A
HSV-TK
Firefly Luciferase
B
WNT-5A 3' UTR GCAAGCAAAAGATCTTGAAATA
miR-129-5P CUUUUUGCGGUCUGGGCUUGC
Luciferase activity (Normalized)
8
6
4
2
0
***
Mock CL
WNT-5A 3'UTR
WNT-5A 3'UTR+NC mimic
WNT-5A 3'UTR+miR-129 mimic
C
VEGF-C 3' UTR AAAAACTGTTGCCACATTAGA
miR-182-5P UUUGGCAAUGGUAGAACUCACACCG
Luciferase activity (Normalized)
20
15
10
5
0
***
Mock CL
VEGF-C 3'UTR
VEGF-C 3'UTR+NC mimic
VEGF-C 3'UTR+miR-182 mimic

## Supplementary Files

This is a list of supplementary files associated with this preprint. Click to download.

- Tables.docx
- Supplementalfolder.pdf